ESL-TR-81-32

ASSESSMENT OF THRESHOLD VISIBILITY —T56 TURBOPROP ENGINES

J.T. SLANKAS
ENVIRONICS DIVISION
ENVIRONMENTAL SCIENCES BRANCH

L.A. MATTISON
SCIPAR, INC
P.O. BOX 185
BUFFALO, NY 14221

J. VAUGHT
DETROIT DIESEL ALLISON, DIV GM
P.O. BOX 894
INDIANAPOLIS, IN 46206

J. STEVENS
USAFOEHL/ECA
BROOKS AFB, TX 78235

JUNE 1981

FINAL REPORT
JANUARY 1980 — MAY 1981

AFESC

ENGINEERING & SERVICES LABORATORY
AIR FORCE ENGINEERING & SERVICES CENTER
TYNDALL AIR FORCE BASE, FLORIDA 32403

NOTICE

PLEASE DO NOT REQUEST COPIES OF THIS REPORT FROM HQ AFESC/RD (ENGINEERING AND SERVICES LABORATORY). ADDITONAL COPIES MAY BE PURCHASED FROM:

NATIONAL TECHNICAL INFORMATION SERVICE
5285 PORT ROYAL ROAD
SPRINGFIELD, VIRGINIA 22161

FEDERAL GOVERNMENT AGENCIES AND THEIR CONTRACTORS REGISTERED WITH DEFENSE TECHNICAL INFORMATION CENTER SHOULD DIRECT REQUESTS FOR COPIES OF THIS REPORT TO:

DEFENSE TECHNICAL INFORMATION CENTER
CAMERON STATION
ALEXANDRIA, VIRGINIA 22314

UNCLASSIFIED

SECURITY CLASSIFICATION OF THIS PAGE (When Data Entered)

REPORT DOCUMENTATION PAGE

READ INSTRUCTIONS BEFORE COMPLETING FORM

1. REPORT NUMBER: ESL-TR-81-32	2. GOVT ACCESSION NO.: AD-A127780
3. RECIPIENT'S CATALOG NUMBER:	
4. TITLE (and Subtitle): Assessment of Threshold Visibility - T56 Turboprop Engines	5. TYPE OF REPORT & PERIOD COVERED: Final Technical Report Jan 80 - May 81
	6. PERFORMING ORG. REPORT NUMBER:
7. AUTHOR(s): John T. Slankas, Maj. USAF; L.A. Mattison; J.M. Vaught; John E. Stevens, Maj. USAF, BSC	8. CONTRACT OR GRANT NUMBER(s):
9. PERFORMING ORGANIZATION NAME AND ADDRESS: HQ AFESC/RDVS Engineering and Services Laboratory Tyndall AFB FL 32403	10. PROGRAM ELEMENT, PROJECT, TASK AREA & WORK UNIT NUMBERS: Program Element 62601F Project 19002027
11. CONTROLLING OFFICE NAME AND ADDRESS: Air Force Engineering and Services Center Tyndall AFB FL 32403	12. REPORT DATE: June 1981
	13. NUMBER OF PAGES: 91
14. MONITORING AGENCY NAME & ADDRESS(if different from Controlling Office)	15. SECURITY CLASS. (of this report): Unclassified
	15a. DECLASSIFICATION/DOWNGRADING SCHEDULE:

16. DISTRIBUTION STATEMENT (of this Report)

Approved for Public Release: Distribution Unlimited

17. DISTRIBUTION STATEMENT (of the abstract entered in Block 20, if different from Report)

18. SUPPLEMENTARY NOTES

Availability of this report is specified on reverse of Front Cover.

19. KEY WORDS (Continue on reverse side if necessary and identify by block number)

Visibility	Photography	C130 Aircraft
Visual Detection	Exhaust Emissions	
Smoke	T56 Engine	
Opacity	Smoke Number	
Photometry	Turboprop	

20. ABSTRACT (Continue on reverse side if necessary and identify by block number)

This report summarizes the results of flight and ground tests performed to determine the threshold visibility of the exhaust plume from a C130H aircraft as a function of Smoke Number. The report first addresses the deficiencies of the present Smoke Number standard and the consequent necessity to correlate visibility with Smoke Number experimentally. Measurements of opacity (both by visual observation and by photometric techniques) and of smoke number are presented followed by analyses of the data. A Smoke Number of 48 was determined to be a conservative estimate of the threshold for exhaust plume visibility.

DD FORM 1 JAN 73 1473 EDITION OF 1 NOV 65 IS OBSOLETE

UNCLASSIFIED

SECURITY CLASSIFICATION OF THIS PAGE (When Data Entered)

PREFACE

This final report was prepared by HQ AFESC Engineering and Services Laboratory, Tyndall AFB, FL. The report covers Air Force and contractor tests during the period 1 January 1980 through 1 June 1980 and subsequent data analyses during the period 1 June 1980 through 15 May 1981. This work was accomplished under Program Element 6260F, Project 19002027. The project officer in charge of coordinating the test program and analyses was Maj John T. Slankas.

A number of people from both the Air Force and industry made significant contributions: (1) Capt James R. Anderson, 6510 TW/TEES, Test Engineer; (2) Maj Wes Werling, Det 4 2762 LSS, Aircraft Pilot; (3) Maj Dave Kender, HQ AFLC, Special Support; and (4) R. L. Johnson, Detroit Diesel Allison, Test Engineer. The organizations and laboratories which participated in the program are listed in Appendix A.

This report reviews the state-of-the-art in understanding the relationship between opacity and Smoke Number. It then presents the test results for both ground and flight tests in making measurements of engine plume opacity and of engine smoke number. Finally, the data are analyzed and a determination of the threshold smoke number for plume visibility is made.

This report has been reviewed by the Public Affairs Office (PA) and is releasable to the National Technical Information Service (NTIS). At NTIS it will be available to the general public, including foreign nationals.

This report has been reviewed and is approved for publication.

John T. Slankas
JOHN T. SLANKAS, Maj, USAF
Chief, Environmental Sciences Branch

Robert E. Brandon
ROBERT E. BRANDON
Deputy Director
Engineering and Services Laboratory

Michael J. Ryan
MICHAEL J. RYAN, Lt Col, USAF, BSC
Chief, Environics Division

(The reverse of this page is blank.)

CONTENTS

CONTENTS (Concluded)

ILLUSTRATIONS

TABLES

1. INTRODUCTION

A study of the exhaust plume visibility of a C130-H aircraft powered by four Allison T56-A-15 engines was coordinated by the Air Force Engineering and Services Center (AFESC). This report documents the work performed in defining test procedures and analyses for visual observations, Smoke Number measurement, and photographic/photometric measurement of the exhaust plume. The overall program objective was to relate Smoke Number measurements with exhaust plume visibility and to determine at what Smoke Number the threshold of visibility occurs. (Smoke Number is the accepted government/industry standard for assessing smoke emissions and will be discussed in detail in Section 3).

The Air Force and The Environmental Protection Agency (EPA) have each published smoke limit specifications based upon measured thresholds of exhaust plume visibility. Although they agree for turbojet and turbofan engines, these differ significantly for turboprop engines. Figure 1 illustrates the Air Force specification (Reference 1) for visible and invisible smoke as it relates to the Smoke Number of an engine measured by the method of SAE ARP 1179 (Reference 2) and using MIL-T-5624 (Reference 3) grade JP-5 fuel. It should be noted that this specification provides a higher Smoke Number goal than does AF regulation 19-1. However, this specification was developed for turboprop engines; AF Regulation 19-1 refers to AFAPL TR-74-64 in which the data and relationships are developed primarily for turbojet engines. (As will be discussed later, turboprop and turbojet engine Smoke Numbers cannot be directly grouped.)

The exhaust diameter of the T56 engine is approximately 50 cm; therefore, as seen in Figure 1-1, the Air Force Smoke Number requirement to insure that the smoke is not visible is approximately 50. For comparison, the 17 July 1973 EPA emission standards for the class "P2" (all turboprop) engine (Reference 4) with an operating shaft horsepower between 4,000 and 5,000 suggests that the appropriate Smoke Number is about 29. Proposed revisions

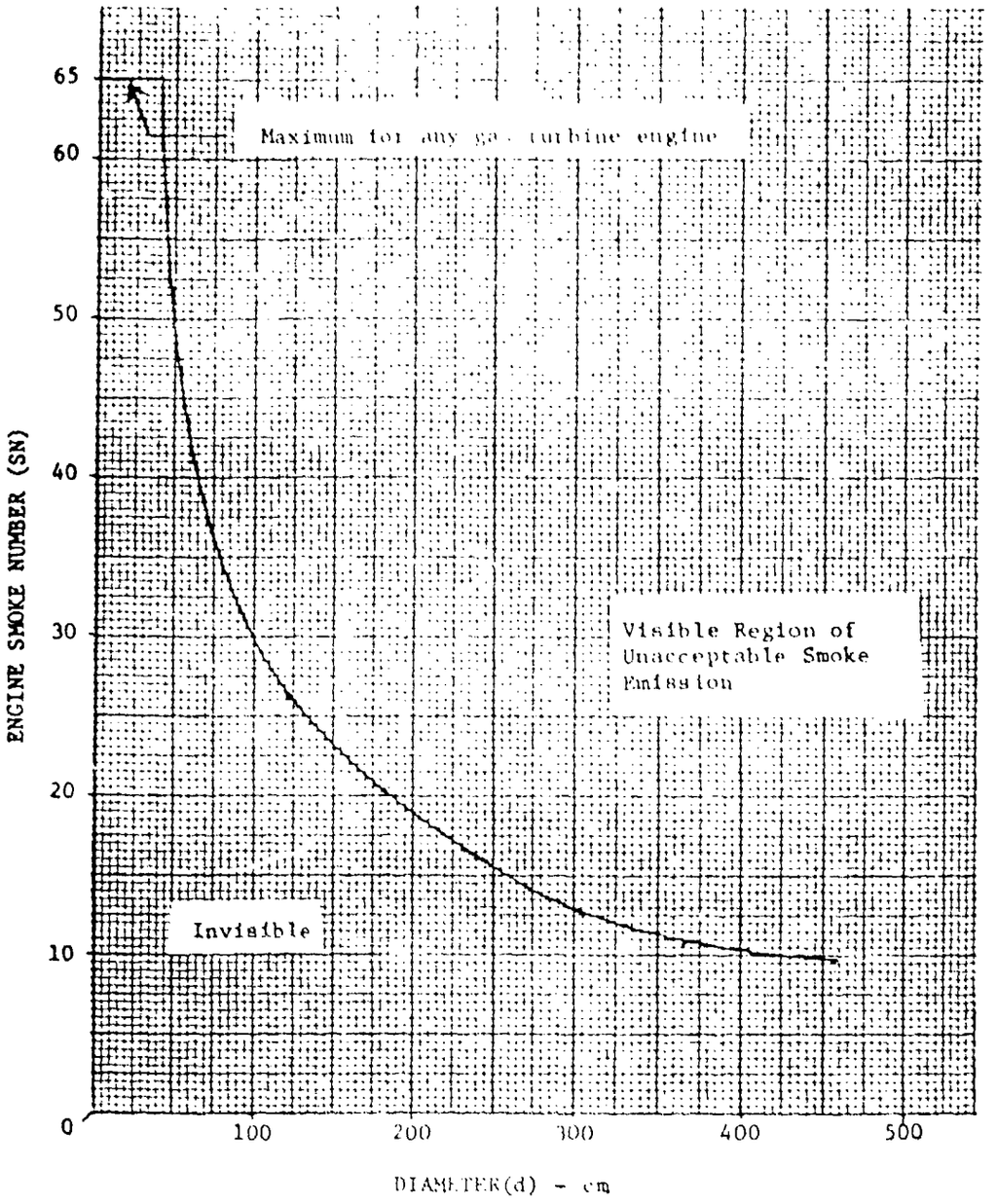

d: Diameter of the vitiated airflow exhaust nozzle at the engine exhaust exit plane. The exhaust exit plane is the first downstream plane, normal to the exhaust stream, that does not contain a solid surface around the stream. For engines with vitiated airflow leaving the engine through an annulus, (d) shall be the diameter of a circle having the same cross-sectional area as the annular exhaust stream.

Figure 1-1. Air Force Visible/Invisible Specification

to the 1973 EPA Standards were issued in 1978 (Reference 5). Under the new specifications, the maximum Smoke Number allowable was restated in algebraic form but was not changed. The 1978 specification requires:

$$SN < 277 \times (r_o)^{-0.280}$$

r_o = rated output power available for takeoff with standard day conditions in kilowats

For the T56 engine, r_o is approximately 3355 kilowats. Therefore the maximum Smoke Number specification is:

$$SN < 277\ (3355)^{-2.80} = 29$$

Each of the above standards claims that it represents the limit of visibility.

The exhaust smoke trails from gas turbine engines expand rapidly from the exhaust diameter from which they exit the engines into a much larger diameter plume. In EPA's Criterion Report (Reference 6), the basis for smoke plume visibility was assumed for simplicity to be the transmissivity of the exhaust gases taken at "the diameter of the engine core flow at the exit plane." The relation between actual aircraft exhaust plume visibility and engine exhaust Smoke Number was neither established nor proven in their report. The simplifying assumption using the exhaust diameter transmissivity was therefore not validated for cases of real aircraft and engines. In fact, considerable evidence exists to prove that transmissvity at the engine diameter is not a valid predictor of plume visibility and that the relationship between jet plume visibility and engine exhaust Smoke Number is complex. This relationship has been defined for jet engines in a program conducted for the USAF by Lockheed Palo Alto Research Laboratory (Reference 7). In this program the turbulent mixing of turbojet engine exhaust with the ambient air was defined, modeled, then correlated experimentally with actual aircraft plume visibility.

Studies of smoke trails from the turboprop engines have led to the conclusion that the engine exhaust becomes part of a complex fluid dynamic system. Almost as soon as it exits, the engine exhaust is mixed into the propeller stream, which is, in turn, influenced by other aerodynamic forces created by the winds and fuselage. This system is illustrated in Figure 1-2.

As in the Air Force turbojet model, other factors which influence visibility include engine size, power setting, number of engines, and placement as well as aircraft flight speed and altitude, observer position, and exhaust smoke concentration.

The determination of visibility of the exhaust plume from turboprop-powered aircraft is, therefore, a complex problem. EPA has acted conservatively in establishing a smoke standard for turboprop engines without performing the supporting analyses and experimental work to define the actual levels of plume visibility. The conflict of standards beween EPA and DOD has resulted because neither agency has performed the technical work required to determine the true threshold of plume invisibility.

Neither standard is based on quantitative measurement of the light transmission of the smoke plume. Utilizing trained observers and the calibrated photometric techniques discussed in this report has provided a more precise determination of the visible smoke level for input to turboprop engine smoke standards.

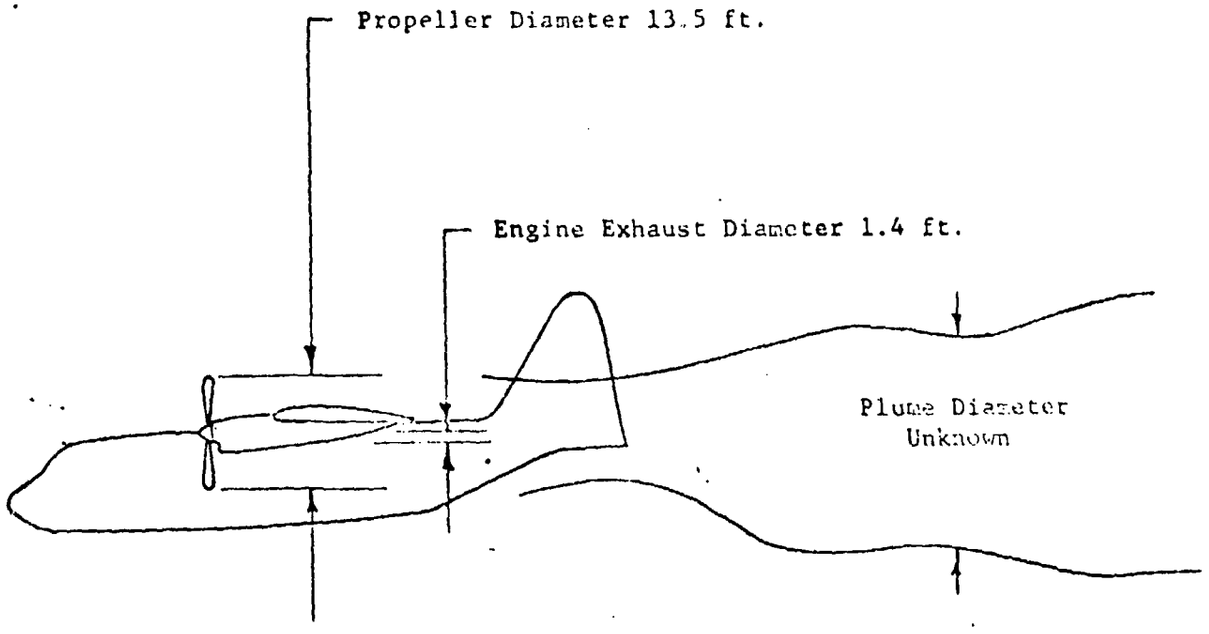

Figure 1-2. Schematic of Exhaust Plume System Observed from Hercules Transport. System Consists of Engine Exhaust Stream. Propeller Stream, and Diluted Exhaust Plume which is Influenced by Wakes from Aircraft.

2. SUMMARY AND CONCLUSIONS

The results of the flight and ground testing performed to determine the threshold of visibility of the exhaust smoke plumes from a C-130H, powered by T56 turboprop engines are reported herein. The exhaust plume visibility in flight was measured photometrically and observed by trained smoke observers. During ground testing, engine runs were made at the same power points used during the flight observations. Smoke plumes from the ground runs were measured, using Society of Automotive Engineers ARP 1179, observed and measured photometrically.

To determine the necessity for making the above tests, a study of the optical characteristics of smoke plumes, and of aircraft engine exhaust plume visibility measurements was made. The results of this study, of the experimental smoke visibility tests of the C-130 transport, and the analysis of the data have led to the conclusions stated below.

a. The analytical studies which preceded the experimental testing confirmed that the determination of exhaust plume visibility and its relation to Smoke Number in the engine exhaust is a complex procedure, depending on a number of different parameters, many of which are poorly defined. Therefore, the only accurate way to determine the threshold of visibility with Smoke Number is by experimental measurement.

b. Contrary to the situation which exists for jet propelled aircraft, prior to these tests, neither data nor mathematical models existed which could be used to establish a Smoke Number standard for turboprop engines.

c. Smoke observations made by trained observers indicated that the EPA standard was overly conservative. Ground runup opacities did not exceed 10 per cent with either JP-4 or JP-5 fuel, under any power condition. Inflight emissions were only visible during approach flybys and turn phases of the test. At no other time did the emissions add to the aircraft visibility.

Exhaust plumes viewed at a perpendicular angle (90° angle between observer-line-of-sight and exhaust plume) were not visible.

d. However, the trained observers could not produce data of sufficient accuracy to define the threshold of visibility during flight.

e. The analysis of the photometric data taken during the flight tests showed that the threshold of visibility was at engine SN = 48.

f. The photometric data analysis also showed that measurement of the exhaust plume transmission of aircraft engines should be made at right angles to the plume, and with a uniform background. This agrees with the conclusions of Hoshizaki, who studied jet plumes (Reference 7).

The experimental and analytical work accomplished during this program was directed toward determining the threshold of visibility and Smoke Number to visibility correlations for the C130 transport and the T56 engine. No work was done to include other engine sizes and propeller-airframe combinations which could be used to generalize the information produced. It is recommended, therefore, that additional work be performed to include various engine sizes, various applications, the study of turboprop exhaust plume aerodynamic performance, and the construction of a mathematical model which can predict visibility threshold levels. The beneficial result would be the capability to accurately predict the exhaust plume threshold of visibility and the associated engine Smoke Number which will meet tactical and aesthetic requirements.

3 TECHNICAL DISCUSSION

The determination of the visibility/invisibility of gas turbine engine plumes is a complex problem. To understand the issues, one must first define plume opacity and determine the factors affecting opacity in plumes. Next, one must study the parameters affecting the optics of aerosols. Then, one needs to apply this understanding to the particular case of aircraft plumes, determining first the factors affecting plume opacity, and then finding how these interplay with Smoke Number. Finally, one must conclude how all the above pertain to the particular case of turbroprop engine plume visibility.

3.1 PLUME OPACITY

When gases are discharged into the air, their plumes are often visible as they contrast against the background, being either considerably lighter (greater luminance) or darker (less luminance). Light interacts with a plume because of absorption and scattering.

The transmittance is defined as:

$$\% \, TR = \frac{I}{I_o} 100 \qquad (3\text{-}1)$$

where I is the intensity of the light passing through the plume
I_o is the intensity of the light entering the plume

Opacity is defined as

$$\% \, OP = 100 - \% \, TR \qquad (3\text{-}2)$$

Thus a transparent plume has 100 percent transmittance and 0 percent opacity; a totally opaque plume has 0 percent transmittance and 100 percent opacity.

Normally transmittance lies somewhere between these extremes and follows Bougher's (Beer-Lambert) Law:

$$I = I \exp(-bx) \tag{3-3}$$

where b is the extinction coefficient due to gases and aerosols in the plume
x is the thickness of the plume.

Generally the extinction coefficient is represented as the sum of several components:

$$b = b_1 + b_2 + b_3 + b_4 \tag{3-4}$$

where b_1 is the component due to light scattering by aerosols
b_2 is the component due to light scattering by gas molecules
b_3 is the component due to light absorption by gases and vapors
b_4 is the component due to light absorption by aerosols

As mentioned earlier, the plume is visible because it contrasts with the background. The luminance contrast is defined as:

$$CP = \frac{B_p - B_b}{B_b} \tag{3-5}$$

where B_p is the luminance of the plume
B_b is the luminance of the background

The luminance of the plume, however, is directly related to that of the background:

$$B_p = B_b \times T + B_{so} \tag{3-6}$$

where T is the fraction of light transmitted through the plume

B_{so} is the luminance seen by the observer due to scattering

The luminance contrast is thus given as

$$CP = T - 1 + \frac{B_{so}}{B_p} \tag{3-7}$$

If we have an absorbing plume (the general case and certainly the case for aircraft plumes), B_{so}/B_p approaches zero; and the contrast is always negative. A contrast of -0.50 therefore indicates a transmission of 0.50, or a transmittance of 50 percent, a contrast of -0.05 indicates a transmission of 0.95, or a transmittance of 95 percent. Thus a contrast map can provide a quantitative analysis of the plume.

3.2 PARAMETERS AFFECTING PLUME OPACITY

The interaction of aerosols with light is a complex phenomena that depends, often in a nonlinear fashion, on such parameters as (Reference 8):

(a) wavelength of the light

(b) size distribution

(c) refractive index (including its complex part, if any) and its size variation

(d) particle shape and physical structure and orientation with respect to the sight path, and their size variation

(e) the variation of b through d along the sight path and in time.

These parameters and how they interact with and affect the components of the extinction coefficient given in Equation (3-4) require examination.

Light interacts with particles in the plume (from molecular size up) as a result of the electromagnetic wave nature of the light and the charge distributions in matter. Particles which are small relative to the wavelength experience the same electromagnetic field throughout. This establishes a dipole in each particle that is a function of its polarizability. As the field varies in time, so does the dipole; hence it emits radiation (all oscillating dipoles do). This emission of light results in the removal of radiation from the incident beam and in the redirection of the radiation in the characteristic dipole pattern. Particles in this size range are said to be in the Rayleigh range (i.e., the particle diameter is less than approximately one-fifth the wavelength, 0.1 μm, for visible light). In this range the scattering component of the extinction coefficient decreases with the sixth power of the decreasing particle diameter -- b_2 is thus negligible in Equation (3-4). The cross-section for absorption, on the other hand, is a volume effect and thus decreases with the third power of the decreasing diameter. (Reference 9)

Hence absorption is the dominant mechanism in the Rayleigh range, and extinction coefficients for absorbing particles will be greater than those for nonabsorbing particles of the same size by roughly a minimum of one order of magnitude. (Reference 10)

Absorption by gases is well understood and is found to be small, if not negligible, in essentially all cases dealing with predominantly aerosol pollutants. Charlson (Reference 8) has examined the case for NO_2 (the only absorbing gaseous species present in optically significant quantities) in auto exhausts. He suggests a typical ratio $b_1/b_3 = 7$ at 500 mm and 10 at 550 mm

based on work of Charlson and Alquist. (Reference 11) Thus, even in a worst case conservative situation, absorption by gases remains small.

As the particle size increases and the aerosol particles become large in comparison to the wavelength of light, the electromagnetic field no longer remains approximately the same across the particle diameter. Mie was the first to describe this situation from a theoretical viewpoint and developed a series of equations to model the scattering behavior (Reference 12). An excellent discussion of these results, called Mie theory in honor of its developer, is given by Vande Hulst (Reference 9). These relationships describe the process of scattering for particles of any size, even in the Rayleigh range, and show a complex character for the solutions where particle size is approximately equal to or greater than the wavelength. This complexity results from the interference of the interacting waves and exhibits strong maxima and minima (structure) as a function both of particle size and of detection angle.

If, however, a distribution of particle sizes is considered, much of the complexity disappears as individual maxima or minima are averaged out (extrema are a function of particle size). Nevertheless, the interactions of particles whose sizes are approximately equal to the wavelength are found to be much larger than for other sizes, and often predominate. As an example, a study was conducted where the scattering coefficient per log diameter interval was calculated (for a measured size distribution in Los Angeles smog) as a function of wavelength. Particles in the narrow range of sizes, 0.2 μm particle diameter < 1.0 μm, accounted for almost all the scattering component in the smog aerosol (Reference 13). Hoshizaki etal. (Reference 7) have made extensive studies examining rocket exhaust plumes which typically scatter rather than absorb light. They find this same behavior. If the aerosol is composed of particles much smaller or much larger than the wavelength of light, the optical signature greatly decreases. Also, they find that if the total particle mass is held constant while the particle diameter is varied,

the combined changes in scattering cross-section and number density result in a maximum scattering coefficient near 1.0 μm. The scattering coefficient is found to be an order of magnitude less for 0.1 μm and 10 μm diameter particles.

The Mie formulas can be used to calculate the optical extinction cross-section (defined by the ratio of the total power dissipated, i.e., power scattered and absorbed, to the incident illumination intensity). The extinction cross-section, C_E, is expressed in terms of the Mie scattering coefficients a_m and b_m by the following relationship:

$$C_E = \left(\frac{\lambda}{2\pi}\right)^2 \sum_{m=1}^{\infty} (2m + 1)\ (\mathrm{Re}\ a_m + b_m) \tag{3-8}$$

where λ is the wavelength and Re signifies the real part. Similarly the cross-section, C_s, for scattering is defined by the ratio of the scattered power to the incident illumination intensity and can be expressed by:

$$C_s = \left(\frac{\lambda}{2\pi}\right)^2 \sum_{m=1}^{\infty} (2m + 1)\ (|a_m|^2 + |b_m|^2) \tag{3-9}$$

The absorption cross section, C_A, can easily be found from the known relationship

$$C_E = C_S + C_A \tag{3-10}$$

Hence, knowing the particle's refractive index, size, and illumination wavelength enables the determination of the cross sections for extinction, for scattering, and for absorption.

Investigations have shown that refractive index, especially the imaginary part, can significantly affect extinction cross-sections both in magnitude and in interface structure. Faxfog (Reference 10) has examined the variation in

extinction cross-section with particle diameter as refractive index is varied (λ = 0.6328 μm). Indices used included those for iron (m = 1.51 - 1.63i), lead (m = 2.01 - 2.48i), graphite (m = 2.50 - 0.75i), polystyrene (m = 1.595), sulfuric acid (m = 1.40), and water (m = 1.33). For particles above 0.3 μm diameter, extinction cross sections were within the same order of magnitude, but for particles below 0.3 μm the cross sections for optically absorbing spheres were more than an order of magnitude larger than for transparent spheres.

No interference structure in plotting the extinction cross section as a function of the particle size is observed for particle sizes in the Rayleigh range. This situation, however, changes as the particle size increases to a magnitude similar to the wavelength. For transmitting particles (extinction cross-section and scattering cross-section equal), pronounced structure exists with maxima and minima in the cross-section as a function of particle size; for particles (extinction cross-section equal to the sum of scattering cross-section and absorbing cross-section), little structure exists--it has been damped out.

Wittig et al. (Reference 14) have examined the effect of adding an abosrbing component to the refractive index. They find that the interference structure has been smoothed out for absorbing particles although the general shape of the cross-section curves for absorbing and nonabsorbing particles remains the same. Work by Roessler and Faxfog (Reference 15) further supports these findings. They find that for absorbing particles the specific extinction coefficient (extinction coefficient per unit mass) peaks at a particle diameter near the incident light wavelength and then rapidly decreases as particle size is increased. In the Rayleigh range, the absorbing particles follow the expected third power dependence on size.

3.3 AIRCRAFT PLUMES AND OPACITY

The mass emissions and particle size data for turbine engine exhausts have been measured now in a number of different investigations. (References 16, 17, 18) Although relatively wide variations are found, the results are consistent enough that certain generalizations can be made.

a. Size distributions are not necessarily simple in structure. Champagne (Reference 19) reported a bimodal size distribution with particles grouped in the submicron region (consisting over 50 percent or more by weight and primarily responsible for plume visibility) and in the region of 1-15 μm. Other investigators have found that the submicron size distributions are also not simple.

b. Particle size number concentration appears to increase as particle size decreases (indicating a particle growth mechanism through carbon agglomeration).

c. Over the range of measurement (0.01 μm and larger), the geometric mean size ranges from 0.04 μm - 0.08 μm depend on the engine power setting. Standard deviation for a representative distribution is approximately 1.7.

d. In contrast to number distributions, volume distributions appear to have a pronounced peak in the 0.05 μm - 0.5 μm range. (Reference 17)

McDonald (Reference 20) was one of the first investigators to examine aircraft exhaust plume visibility. He concluded that a large fraction of all emitted carbon leaves the tailpipe in the form of carbon particles of only a few hundred Angstrom units diameter and that soot formation takes place primarily in the wake, aft of the engines. Results of Stockham and Betz (Reference 21) further support these conclusions. They found the geometric mean particle diameter to be 0.052 μm at the exhaust and to increase in size to 0.13 μm ten nozzle diameters downstream. Exhaust particles had a lacy agglomerated

structure and were characterized as carbon flocs. This is consistent with their earlier assessment that the extinction of light by turbojet engine smoke is due to 11 percent scattering and 89 percent absorption of light, i.e., primarily an absorbing plume. The essentially carbonaceous content of aircraft exhaust particulates has been noted by a number of investigations, including a recent detailed characterization of the chemical composition of gas turbine engine exhaust particulates. (Reference 22)

Although carbonaceous in nature, particulates are not completely composed of carbon, but can have significant amounts of other elements, especially hydrogen and oxygen. Furthermore, agglomeration mechanisms generally result in irregularly shaped particles instead of smooth spheres. (Irregularly shaped particles, have been found to damp the interference structure and smooth the extinction cross-section curve as a function of size.) (Reference 23).

This lack of knowledge on the structure and composition of the exhaust particulates presents two problems. The first is how to account for shape factors and their effect with particulate size distributions on the extinction cross-section. The second is what index of refraction should be used (Reference 24). As discussed previously, size distributions are poorly defined; and measurements that are made give an effective size. Hence, only estimates of an "effective" size distribution can be made. Also, as discussed earlier, the index of refraction, especially the imaginary part, has a major effect on the opacity of small particle plumes. Ensor and Pilat (Reference 25) have demonstrated significant changes in what is essentially the extinction cross-section for plumes composed of submicron particles with a geometric mass mean radius near 0.1. They have also determined optical parameters for a number of different sources. They have found a variation in extinction coefficient greater than a factor of ten when they include fly ash as well as various black smoke sources (absorbing plumes); and even for the various black smoke sources they find a variation greater than a factor of

three. They attribute these variations to size distribution, particle density, and refractive index changes.

In later work Thielke and Pilat (Reference 26) have demonstrated a method for characterizing the relationship between particulate mass concentration and light transmission when the particle size distribution deviates from the log-normal model. This requires knowledge of size distribution, refractive index, and incident light wavelength. This, or a similar method is needed to properly characterize an aircraft plume. The conclusion, therefore, is that light transmission and smoke concentration cannot directly be related without significant error, unless additional physical parameters are known.

3.4 SMOKE NUMBER.

Traditionally, three different techniques have been available to quantify particulate emissions: gravimetric mass, plume visibility, and stained filter. Smoke Number utilizes the stained filter technique and, in a sense, relates mass and opacity. Smoke Number is a dimensionless term quantifying smoke emissions from gas turbine engines during ground test and is used as the current government/industry standard. The procedures for measurement are well-defined and standardized in ARP 1179. (Reference 2) Smoke Number (SN) is defined by the following equation:

$$SN = 100 \left(1 - \frac{R_s}{R_w}\right) \tag{3-11}$$

where R_s = reflectance of the soiled filter
R_w = reflectance of the unsoiled filter

when the filter loading, i.e., the mass of gas passed through the filter paper per unit area, is 0.023 lb/in.^{2} or 1.62 g/cm^2. Thus Smoke Number increases with smoke density and is rated on a scale from 0 to 100.

Wood (Reference 27) has reviewed the correlations between smoke measurements and optical properties of jet engine smoke. The projected extinction area of the smoke particles is given as $S_p(W_e/\rho_e)W$ where S_p is the specific particle extinction area (extinction coefficient per unit mass), w_e is the mass of smoke particles per unit exhaust gas, ρ_e is the density of engine exhaust gas, and W is the mass of engine exhaust gas. The extinction area is then used in the development of an expression to relate the soiled area (A_s) on the filter paper to the unsoiled area ($A-A_s$):

$$\frac{A_s}{A} = 1 - \exp\left\{- S_p \frac{W}{A} \frac{W_e}{\rho_e}\right\} \tag{3-12}$$

Assuming that the reflectance of the soiled filter can be expressed as the area-weighted sum of the unsoiled area ($R = R_w$) and the soiled area ($R = 0$, assuming total absorption by the particles), Equation (3-12) may be expressed as:

$$\frac{R_s}{R_w} = \exp\left\{- S_p \frac{W}{A} \frac{W_e}{\rho_e}\right\} \tag{3-13}$$

Shaffernocker and Stanforth (Reference 28) measured reflectivities against a gray background for jet engine mass emissions. Making the correction for background and applying the relation given in Equation (3-13) shows that a fit with the data only exists in a narrow range of reflectance ratios R_s/R_w from 1.0 to 0.8. However, Wood then used a concept introduced by Stockham and Betz (Reference 21) to incorporate an exponential factor in Equation (3-13). When this is done, the equation has the form:

$$\frac{R_s}{R_w} = \exp\left\{- S_p \frac{W}{A} \frac{W_e}{\rho_e}\right\}^b \tag{3-14}$$

where b and C are both constants. Good agreement with the experimental data is found assuming $S_p = 8.64 \times 10^4$ cm^2/g, b = 0.48 and C = 3.14 over a range of reflectance ratios R_s/R_w less than 0.6, i.e., heavily stained. The range between the two sets, i.e., $0.6 < R_s/R_s < 0.8$, can be fit by a smooth curve.

These relationships between Smoke Number and mass loadings, especially those for higher Smoke Numbers ($R_s/R_w < 0.6$), have a number of limitations. Particle reflectives are assumed to equal zero, i.e., totally absorbing; the optical nature of the particles is assumed to be unaffected by the filtration process; finally, a multiparameter curve (S_p, b, and C all are allowed to vary) is fit over a limited amount of data. In fact, one later research group has concluded that Smoke Number measurements do not correlate with gravimetric measurements. (Reference 29)

Relationships between Smoke Number and exhaust transmittance have also been examined. Work done by Champagne (Reference 19) to define smoke plume visibility as a function of smoke plume visibility was incorporated into AFAPL TR-74-64 (Reference 30) which, in turn, is quoted by Air Force Regulation 19-1, governing Air Force smoke goals. Essentially Champagne applied an equation developed by Ensor and Pilat (Reference 31):

$$\frac{I}{I_o} = \exp\left\{-\frac{L\,W_e}{K\,\rho} \times 10^{-3}\right\} \qquad (3\text{-}15)$$

where I_o = incident light
I = transmitted light
L = path length for attenuation
ρ = average particle density
K = a coefficient (units of cm^3/m^2) determined from curves as a function of particle size distribution, index of refraction, and light wavelength.

Using I/I_0 = 0.95 and 0.98, assuming the particle size distribution given by Stockham and Betz (Reference 21), taking the K value corresponding to this distribution (assuming also a value for the index of refraction which has a strong affect on K), and taking ρ = 2.0, Champagne generated a transition regime between invisible plumes and visible plumes. The lower boundary of this regime corresponding to the I/I_0 = 0.98 has been incorporated into Air Force Regulation 19-1 as the Smoke Number goal as a function of plume depth at the nozzle (the nozzle diameter). Over the range of particle sizes and possible refractive index values which aircraft exhaust particulates may have, the K value <u>can</u> change substantially, although the value chosen by Champagne does appear to be conservative at the lower boundary of possible values, and hence results in maximum opacity) ($K = 1/\rho S_p$; i.e., it is inversely proportional to the product of density and specific extinction coefficient). Over the range of geometric mean particle sizes and standard deviations found to be typical for aircraft emissions, K values can change by over 30 percent; more importantly, over the possible ranges of refractive index values, K values can change even more. Hence, phenomena such as agglomeration of carbon particles into soot flocs, cannot be trivially assessed in their effects on plume visibility.

3.5 TURBOPROP VISIBILITY.

As shown in the previous discussions, determination of plume visibility and its relation to Smoke Number is a complex procedure, depending on a number of different parameters. These parameters are poorly defined, which leads to the conclusion that actual measurement of the plume visibility and Smoke Number over a range of operating conditions is the only <u>accurate</u> way to determine the threshold of visibility with Smoke Number.

Additional considerations also must be made concerning whether engine exhaust diameter is a reasonable parameter in the USAF Smoke Number goal. Engine exhaust diameter is determined by the type of cycle as well as mass flow. Turbojet engines, for example, use small sonic, choked nozzles;

turboprop engines require large, low velocity turbine exhaust. This characteristic exhaust diameter is defined for two different cycles of 501 (T-56) engines in Table 3-1. The first engine shown, the 501-022A, was designed to operate at 320 knots air speed between 15 and 30,000 feet altitude, and has a small amount of thrust recovery from the exhaust. The second example shows how the 501 engine would be designed if power recovery in the turbine were to be maximized for low speed operation, without thrust recovery. The Smoke Number required by the Military smoke standards is also given. Table 3-1 shows that the same gas generator (the same mass flow, cycle temperature and pressure ratio) can require an exhaust nozzle diameter which varies from 17.2 inches to 29.8 inches depending entirely on the application cycle chosen. Furthermore, the table also shows that the same gas generator would have to meet Smoke Numbers which vary from 35 to 54 depending on the cycle and consequent exhaust diameter. Considering the fact that each of the two example engines produces the same mass of exhaust, it can be seen that nozzle diameter alone is not an acceptable parameter for smoke control. An invisibility criterion which uses exhaust nozzle diameter alone therefore can lead to a wrong conclusion.

TABLE 3-1. ENGINE EXHAUST ENGINE CYCLE RELATIONSHIP FOR 501 SERIES III ENGINES

501 Engine Variant	Typical Aircraft Application	Nozzle Area	Nozzle Diameter	Reference Military Specification	Required Smoke No.
501-022A	320 Knots Transport	232.7	17.2 (45.7 cm)	MIL-E-8953A	54
Free Turbine with exhaust diffuser	Low Speed Transport	700	29.8 (75.8 cm)	MIL-E-8593A	35

Additionally, work done on turbojet powered aircraft plumes has further demonstrated the weakness of using present Smoke Number criteria (Reference 7). In this Air Force-sponsored program, a model was developed which (1) defines the exhaust plume properties at the engine exhaust; (2) computes the

engine wake and the turbulent mixing of the wake with ambient air; (3) computes the smoke concentration in the wake and the local extinction coefficient; (4) determines contrast; and (5) assesses threshold smoke criteria. Results were compared with data and agreement ranged from good to poor.

As part of this Jet Plume program, both USAF and EPA jet engine smoke standards were examined. These were found to be "adequate and may be somewhat conservative in terms of plume visibility." The explanation offered for this conclusion was that Champagne did not consider the effect of nozzle exhaust gas density, i.e., (Reference 19) in his correlation of Smoke Number to transmittance. In the hot exhaust, density is much lower than the standard temperature and pressure conditions. This results in Champagne's curves being too low.

Other conclusions were that the Air Force Goals are "fortuitious" and "smoke standards for the esthetic nuisance case which correspond to plume invisibility at or near the nozzle exit would also be adequate for the tactical case."

To be sure that the Air Force "Jet Plume Visibility" report had been interpreted correctly, this program was discussed with Dr. W. S. Blazowski, who was the USAF project officer, and Mr. H. Hoshizaki, Lockheed Palo Alto Research Laboratory, who was technically responsible for the work. It was found that the program was directed toward smoke detection from turbojet-powered aircraft, but not to turboprops and that no plume model existed for turboprops.

In summary, it was found that while the USAF and EPA smoke standards for turbojet engines were conservative and the USAF jet goals were "fortuitous," no such program or model existed which could be applied to smoke from turboprop aircraft. Furthermore, no valid bases existed to predict a turboprop smoke standard with a high degree of confidence.

4. TEST PLAN AND PROCEDURES

The currently accepted standard relating gas turbine engine smoke emissions and exhaust plume visibility is Smoke Number. However, as pointed out in the previous chapter, the relationship between visibility and Smoke Number is an indirect, empirically derived correlation that contains a number of assumptions. The net result is that Smoke Number often becomes more a qualitative than an actual quantitative guideline for exhaust plume visibility. To resolve this problem for the specific case of the T56 turboprop engine, a series of tests was conducted on a C130H transport at the Air Force Flight Test Center, Edwards AFB, California. The objective of these tests was to define the Smoke Number(s) at which the T56 exhaust plume became invisible. The major objective of this test program was to relate the ground test smoke measurement method, SAE Aeronautical Recommended Practice No. ARP 1179, with the in flight exhaust plume visibility from the T56 engine.

Both flight tests and ground runs were conducted at different engine power settings. JP-4 and JP-5 fuel were both used so that a range of increasing Smoke numbers was covered in which the exhaust plume transitioned from appearing invisible to appearing visible. On the ground, both Smoke Number and visibility measurements were made by trained observers and by photometric techniques. During flight tests, only visibility measurements were made.

4.1 FLIGHT TESTS

The flight tests were held at the North Base Runway 06-24 at Edwards AFB. Based on photographic measurement requirements and EPA requirements for observation of visual opacity of smoke missions, the data was collected with the sun at the back of the observers. The flight sorties included normal takeoffs, flybys, and approach and landings using JP-4 and JP-5 fuels. Engine power settings were flight idle, approach, cruise, climb and takeoff power for each fuel type.

Takeoffs and landings were accomplished to and from the west and the flight pattern selected was race track. Figure 4-1 illustrates the flight path and locations of the observers and tracking platforms. The solid portion of the flight paths indicate the location of the aircraft when smoke transmission data were recorded. Point A was an average of 17K ft from Point B and represents the beginning of the inbound portion of the flight path. At airspeeds of 200 to 300 knots (340 to 500 fps) each inbound sequence provided approximately 40 seconds for data collection.

The observers and recording cameras were located on the south side of the runway. Camera #1, mounted on the tracker, was located on the edge of the runway, along with a visual opacity Observer A, as shown in Figure 4-2. Camera #2 was positioned 300 ft offset from the runway, as illustrated in Figure 4-1. Visual opacity Observer B was located on the edge of the runway, approximately 2000 ft west of the cameras. The separate positions were selected to provide slightly different viewing aspects for each observation made. However, the fly-in from Point A at 17K range provided similar viewing aspects for each of the three positions for most of the inbound sequence. For the average flight altitude at 400 ft and track ranges of 17K ft to 5K ft, the observer viewing elevation angles for Observer A and the two cameras were 1.4° to 4.6° and for Observer B were 1.5° and 7.6°.

Data recorded on the aircraft during the flight test included each engine horsepower, fuel flow, torque, turbine in temperature, altitude, airspeed, and aircraft configuration. Ambient conditions at the time of the flight tests (20 May 1980, 0830 hours to 1021 hours), included measured air temperatures of 60°F to 78°F, and atmospheric pressure of 27.51 inches of Hg. The wind speed ranged from 1 mph to 0 mph at a 10° heading. The visibility varied from 45 miles to 35 miles.

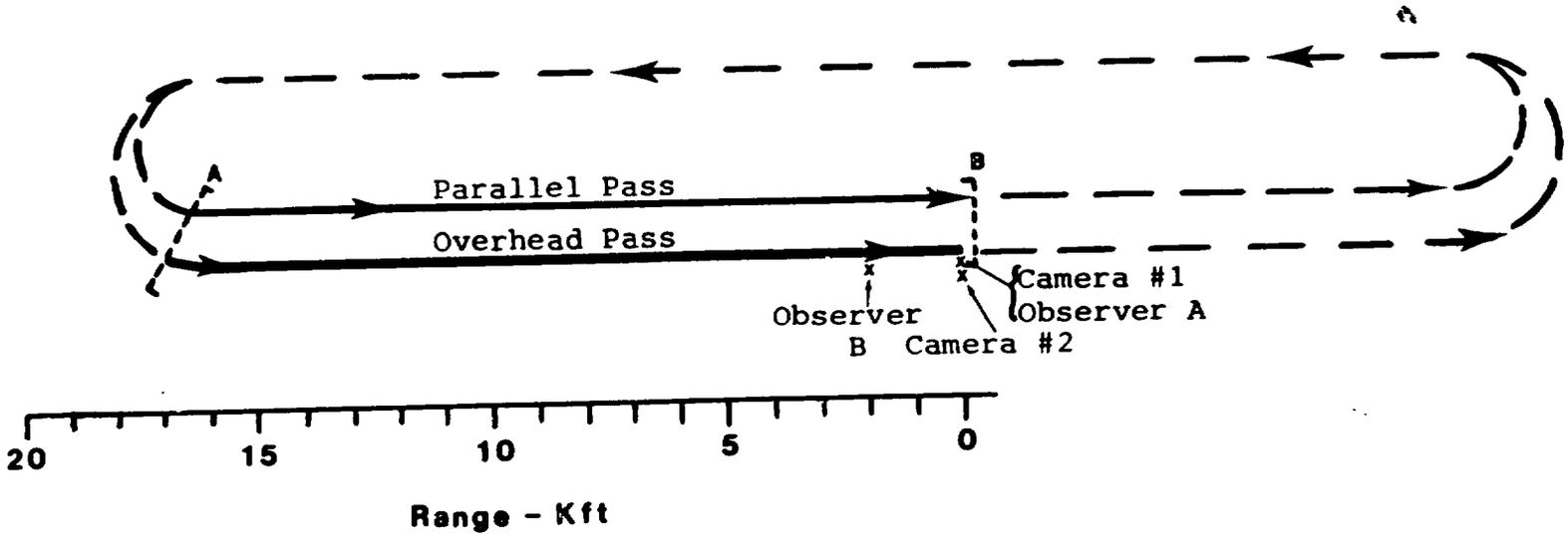

Figure 4-1. C130 Racetrack Flight Pattern

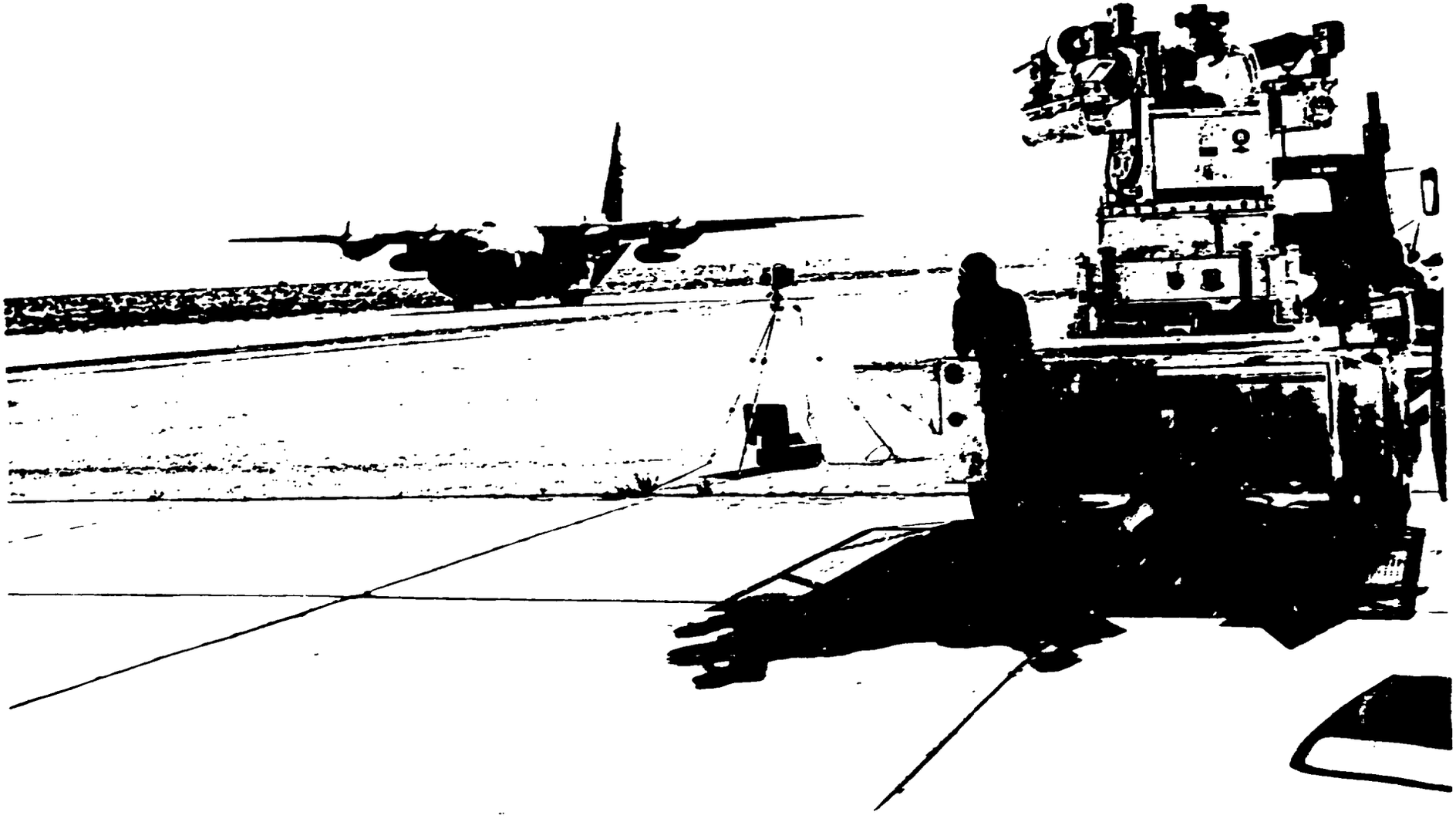

Figure 4-2. C130H On Takeoff Roll During T56 Smoke Tests at Edwards Flight Test Center. Tracker With Camera #1 and Smoke Observer A Are at the Right.

4.2 GROUND TESTS

Ground testing consisted of a run-up of the inboard engines of the aircraft during which engine Smoke Number and exhaust plume visibility were measured over the engine power range. The tests were conducted on a runup pad number 18 on the afternoon of May 20, 1980 from 1352 to 1459 hours. Figure 4-3 shows A/C 1586 during ground test running.

During these tests, the aircraft was faced west so that the sun would be normal to the exhaust streams. Engine number 2 was instrumented for smoke measurement. Engine No. 3 was run at the same power setting to balance thrust on the aircraft. The exhaust plume visibility from both engines operating on both JP-4 and JP-5 fuels was measured by observer and photometric methods. The fuel which was used during the flight and ground testing, was sampled by draining approximately 1 pint from each of the wing tanks.

4.2.1 Engine Smoke Measurements

Four candidate fuels were originally planned for the C130 flight tests: JP-5, JP-4, commercial heptane, and a blend of heptane with JP-4. Materials laboratory tests of these fuels were made to evaluate the smoking potential of each fuel and to determine the blending proportions of heptane/JP-4. ASTM smoke point tests, API gravity, and percent aromatics were used as criteria. The results were predictable. Smoke point ranged from 21.6 mm for JP-5 to 43.4 mm for heptane. A blend of 60 percent heptane, 40 percent JP-4 was selected as the fourth fuel for engine testing.

All four fuels were run in a T56 Power Section on engine Dynamometer tests at the Detroit Diesel Allison factory to determine the Smoke Number (SN) produced by each fuel. The results of these tests were not anticipated. Engine SN did not correlate with ASTM smoke point or fuel hydrogen content - which was contrary to accepted literature results. As shown below, engine SN

Figure 4-3. C130H During Ground Testing at Edwards Flight Test Center. Engine No. 2 was Instrumented for Smoke Measurement. Engine No. 3 Was Run for Thrust Balance.

was 55 and was reduced as expected during running on JP-4, but then it remained constant on the 60/40 heptane/JP-4 blend and even on 100 percent heptane. Consequently, heptane and the heptane/JP-4 blended fuels were dropped from the program.

TABLE 4-1. T56 SMOKE WITH VARIOUS FUELS

Fuel	Engine SN	Smoke Pt.	% Hydrogen
JP-5	55	21.6	14.0
JP-4	46	29.2	14.6
Heptane/JP-4	45	37.9	15.2
Heptane	45	43.4	15.5

While unexpected, the above results still provided the necessary range of Smoke Number based on earlier crude estimations of visibility threshold conducted in-house by Detroit Diesel Allison.

Ground smoke tests were then made at Edwards AFB using JP-4 and JP-5 on a T56-A-15 engine that was the left inboard engine on a C13OH aircraft: Aircraft serial number 73-1586, engine serial number AE 106872. Figure 4-4 shows the ground smoke tests in progress. Engine number 3, the right inboard, was run at the same time to balance thrust on the airplane and help keep the plane stationary. To sample the exhaust, a smoke probe was clamped to the tailpipe of engine No. 2, replacing the aircraft exhaust pipe. The probe was designed for test stand measurement of T56/501 engines and was modified for this test program by adding an exhaust deflector. The probe consists of: seven radial tubes, each with four sampling holes; supporting struts and external shell, a centerbody collector, a clamping ring and an exhaust deflector shield. Each of the 28 sampling holes is located at the centroid of 28 equal areas, so that sampling of the exhaust is representative. The exhaust from

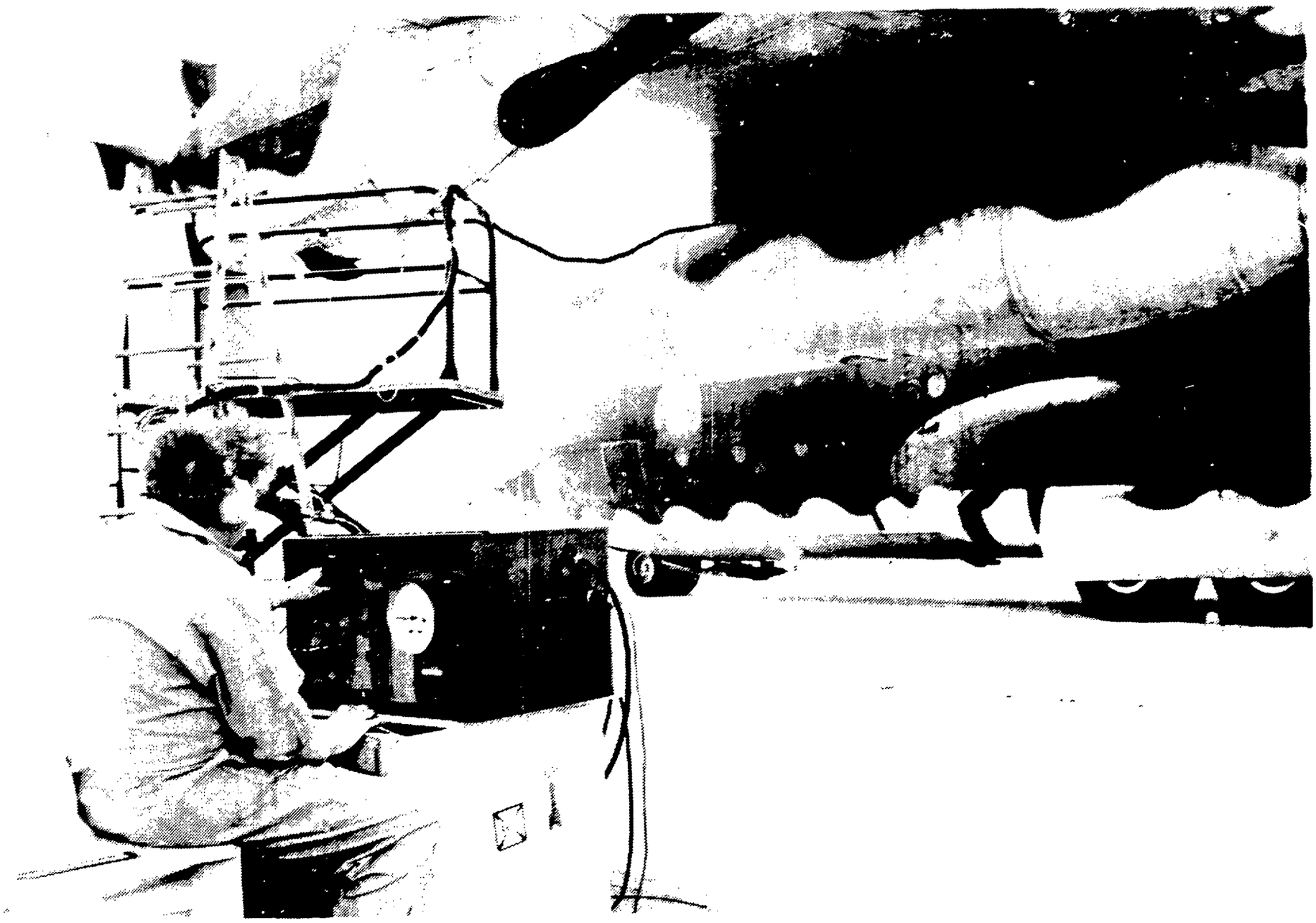

Figure 4-4. Ground Smoke Testing at Edwards Flight Test Center During T56 Smoke Visibility Program

each of the seven tubes is manifolded into a center collector and thence to the sample line, which was heated. The smoke meter, sample line and probe, all conform with SAE ARP 1179, as did all test procedures.

4.3 VISUAL OBSERVATIONS

The USAF Occupational and Environmental Health Laboratory (USAF OEHL) provided two certified visual emission readers for the test series, Capt John E. Stevens, Jr, Consultant Air Resources Engineer, and TSgt John Vlasko, Air Quality Technician. Both Captain Stevens and Sergeant Vlasko held valid certificates from the Texas Air Control Board to conduct visual opacity determinations.

During the flight tests, both observers were stationed on the south side of the runway, approximately 1/4 mile from each other. The aircraft was visible to each observer during its entire rectangular flight pattern, except for a 10-second interval where distant trees blocked the observer's view. With this race track shaped flight pattern, the observers could be perpendicular to the plume at only two points. At these two points, the minimum visual path through the plume could be obtained. At other points in the flight path, the observers always looked through a longer path length of smoke plume.

No difficulty was experienced in keeping the sun oriented in the quadrant of the observer's back. Observer B recorded readings at least every 15 seconds during the entire flight pattern. Observer A was situated next to the photographic equipment and read at 5-second intervals, but only during the approach and flyby phase of each run (Zones A-B on Figure 4-1).

4.4 PHOTOGRAPHIC/PHOTOMETRIC MEASUREMENTS

For photometric measurements, two 35 mm Canon F-1 format cameras were used. Each camera was equipped with a 250-exposure film back, motor drive, automatic

exposure control, and a 100 mm lens with a Wratten No. 8 yellow filter. The photographic film/filter system was designed to obtain a spectral response approximating the eye (photopic). To obtain records of the overall illumination conditions at the time of the test, a SpectraSpot 1/2° Field-of-View photometer was used.

The selection of the photographic film for recording of the photometric data is dependent upon the ratio of the amount of light from the smoke plume to the amount of light from the background (transmission of the plume). For this test, the exhaust smoke plumes were expected to be near the threshold of visibility, i.e., 95 to 98 percent plume transmission, and therefore, the brightness of the plume was expected to be very close to the brightness of the background.

Specification of the film was based on the minimum plume transmission to be measured and the minimum density change on the film that can be measured. The instrument used to measure the film density was a Perkin-Elmer Micro 10 microdensitiometer, which was able to measure density differences as small as 0.02. The plume transmissions that were to be measured during flight tests were expected to be as high as 98 percent. When the smoke plume is photographed, the transmission of the plume is:

$$\text{Transmission of plume} = T = \frac{B_s}{B_o} = 10^{-\Delta D/\gamma} \qquad (4\text{-}1)$$

where B_s is the apparent brightness of the smoke

B_o is the apparent brightness of the background

ΔD is the measured density difference on the film

γ (gamma) is the contrast of the film measured using sensitometric calibration.

Based on B_S/B_O equal to 0.98 and D equal to 0.02, the minimum film contrast, gamma, required for the test was computed from the above formula to be 2.22.

Eastman Technical Plan Film No. EK 2415 has contrast values between 3 and 4. This was confirmed by sensitiometric tests of the film, conducted at OCT's Photographic Laboratory. A file contract of $\gamma = 3.88$ was found from these tests using standard procedures in a Versamat processor at 5 feet per minute with Hunts 500 developer at 79.8°F. Since this film contrast was very good based on the defined requirements, it was selected for the test program.

The proper exposure level during the flight test was required to provide good images for analysis. The primary concerns were: to obtain sufficient density of the sky background on the negative film (the dark smoke will always appear less dense), and to assure that the exposure was at a level where the film is most sensitive to varying image brightnesses so that the analysis software could more precisely calculate the plume transmission. Based on a test series of photographs taken, the above preliminary processing test, the ASA film speed on the automatic exposure controller was set at 80 to produce an expected sky background density on the film of 2.3.

A tracking platform, shown on Figure 4-5, and a conventional tripod were supplied by OTC to record the flight tests. The tracker was a large manually-controlled, motor-driven platform which mounted the 35 mm camera (camera #1) and four 16 mm cameras which were for documentation purposes. Camera #2 was mounted on the tripod. The camera locations are shown on Figure 4-1.

The shutter controls on the two cameras were electrically linked to provide synchronized photographs of the smoke plume. The photographic sequence was started at the beginning of each inbound portion of the C-130 flight at a rate of one frame every 5 seconds.

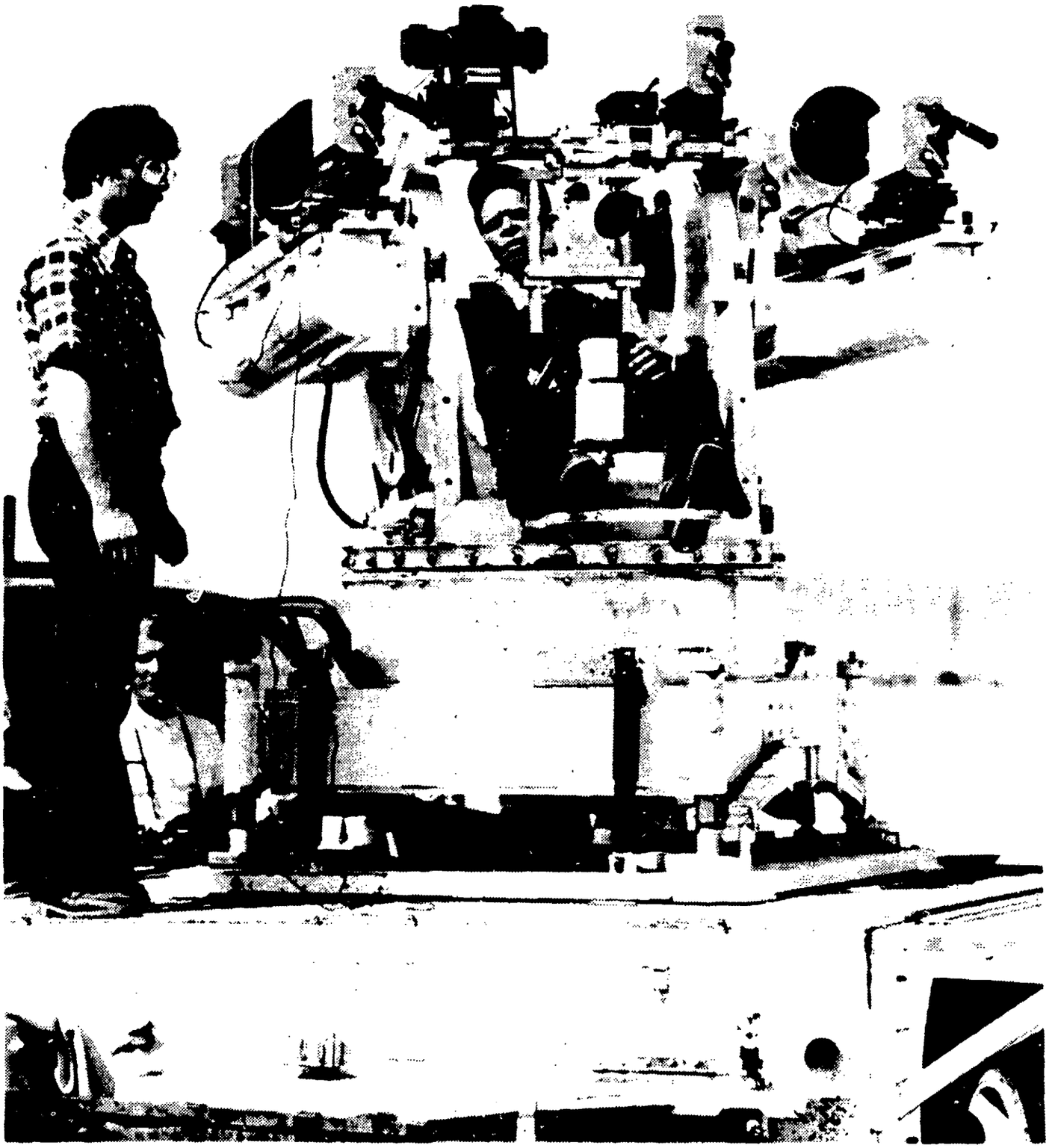

Figure 4-5. Manual Tracker Used in T56 Exhaust Smoke Tests. Canon AE-1 Camera and Various 16 mm Movie Cameras are Shown Mounted

A problem developed with Camera #1 (tracker-mounted) which was not discovered until near the end of the flight sequences. The automatic exposure control on the camera was required to provide proper exposure of the film independent of the varying scene background brightnesses. The camera was mounted on the tracker, however, without covering of the viewfinder on the rear of the camera after the system was boresighted. With sunlight entering the viewfinder, the exposure sensor determined improper camera exposure settings. As a result, the recording film was underexposed and could not be used for data analysis. The second camera at 300 ft offset, however, provided data at similar viewing aspects for a large percentage of the inbound sequence. For example, for the ranges of 17K ft to 15K ft the viewing azimuth difference varied from 1° to 3.5°.

4.5 PHOTOMETRIC DATA ANALYSIS PROCEDURE

The basic photometric analysis scheme is illustrated in Figure 4-6. The film record of the smoke plume during the tests was developed using calibrated photographic processing in an OTC automatic processor. Image analysis was then conducted at SCIPAR by scanning the film with a microdensitometer to convert the image into a digital input for the computer. The computer analysis of the digitized image produced a transmission map of the smoke plume that indicates the ratio of the plume brightness to the brightness of the adjacent sky background.

4.5.1 Photographic Processing

The film was calibrated for sensitivity using the 21-step exposure tablet in a Kodak Model 101 Sensitometer. Blank portions of the test film were exposed so that the step images could be processed with the test images. The exposure and processing of the step tablet provided information necessary to relate the film densities measured to the amount of light that exposed the film. The absolute exposures produced on the film at each step are provided

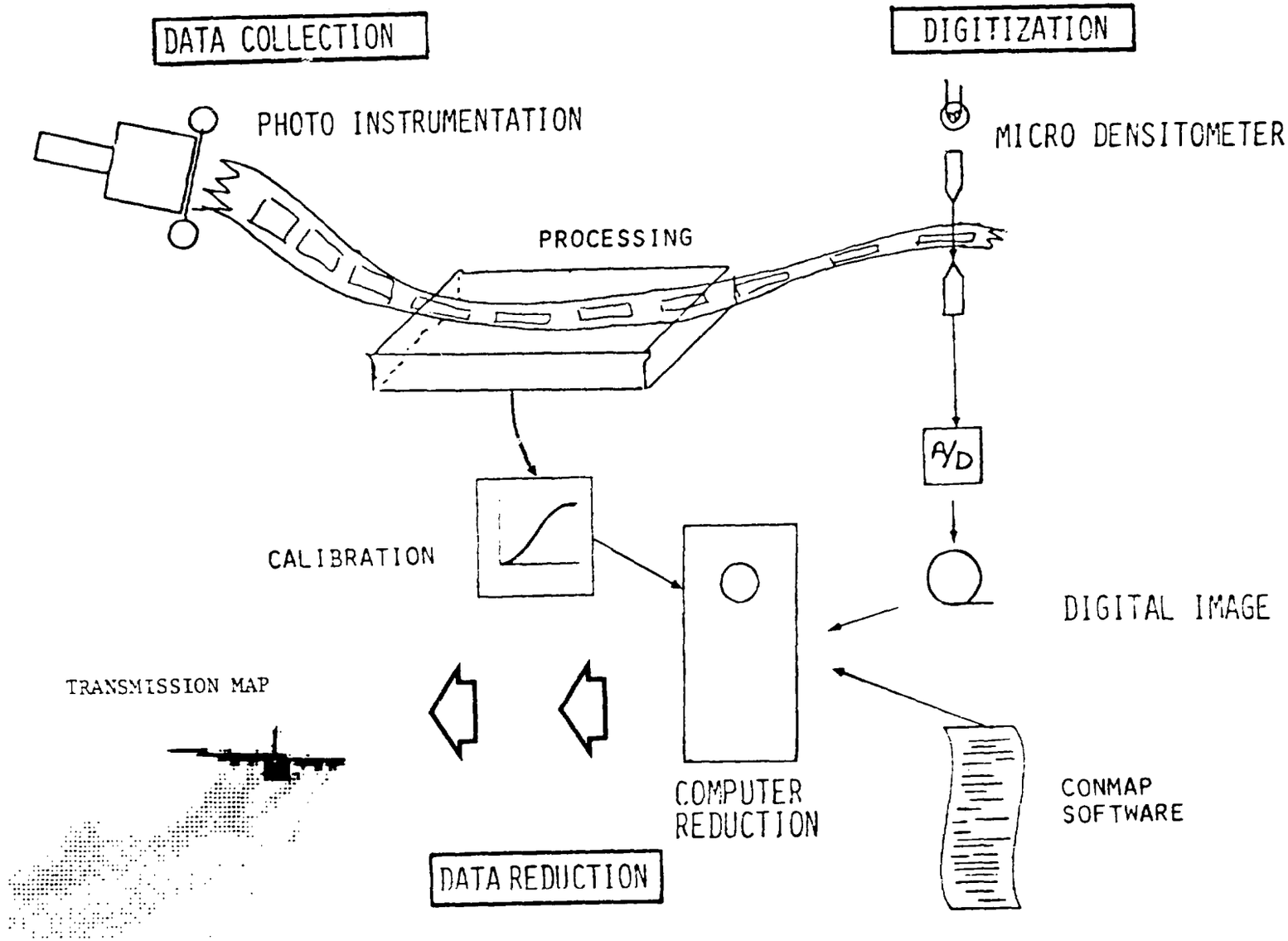

Figure 4-6. Photographic Data Collection/Reduction Flow Diagram

in Table 4-2. Five step tablets were used during processing for evaluation of the film response throughout the development sequence.

TABLE 4-2. ABSOLUTE EXPOSURE AT EACH STEP

STEP	EXPOSURE ($\frac{LUX}{SECS}$)	LOG_{10} EXPOSURE
1	0.0025	-2.82
2	0.0020	-2.70
3	0.0031	-2.51
4	0.0044	-2.36
5	0.0063	-2.20
6	0.0085	-2.07
7	0.0126	-1.90
8	0.0182	-1.74
9	0.0257	-1.59
10	0.0363	-1.44
11	0.0537	-1.27
12	0.0759	-1.12
13	0.1072	-0.97
14	0.1514	-0.82
15	0.2138	-0.67
16	0.3020	-0.52
17	0.4266	-0.37
18	0.6026	-0.22
19	0.8511	-0.07
20	1.2023	0.08
21	1.6982	0.23

The film was processed in a Versamat® processor at 5 feet per minute with Hunts 500 developer at a temperature of 80.8°F. The maximum length of film that could be processed was unlimited. The processing sequence was

completed in less than 2 hours. The imagery processed included approximately 500 frames from the two cameras used in the flight test and 100 frames from the ground test film.

4.5.2 Photometric Analysis Procedure

A Perkin-Elmer Micro 10 microdensitometer and Digital VAX 11//80 Computer System at SCIPAR were used for analysis of the test films. The microdensitometer digitized the photographic images, recording the densities over a matrix of the image on digital tape. The aperture size selected for scanning the image, dependent on the overall image size, was 0.050 mm. The recorded data tape was then transferred to the VAX computer for exposure/contrast analysis and production of plume transmission maps using SCIPAR CONMAP software.

The image location on the film must be identified for input to the microdensitometer since a restricted portion of the film is scanned. Coordinates identifying the location of the smoke plume image and areas of the background sky image on each photographic frame were obtained, using a grid overlay with 1 mm spacings. Using visual examination, the plume image location was identified,using the bottom right corner of each frame as a reference point. The area scanned on each frame containing the smoke plume was a dimension of 5 mm by 6 mm. Within this area the density of the image was measured at 12,000 positions on a matrix with a 50 μm spacing. The scanning sequence utilized for each image provided a specific order in which the data was recorded that allows the computer to reconstruct a map or "picture" of each image. The scanning sequence of the film examined used 120 scan lines each containing 100 density readings. The relative position of each of the readings (pixels) on the images is illustrated in Figure 4-7.

Analysis of the image densities requires input of the sensitiometric characteristics of the film. The density of each of the 21 steps from the five sensitiometer exposures processed with the images was read using the

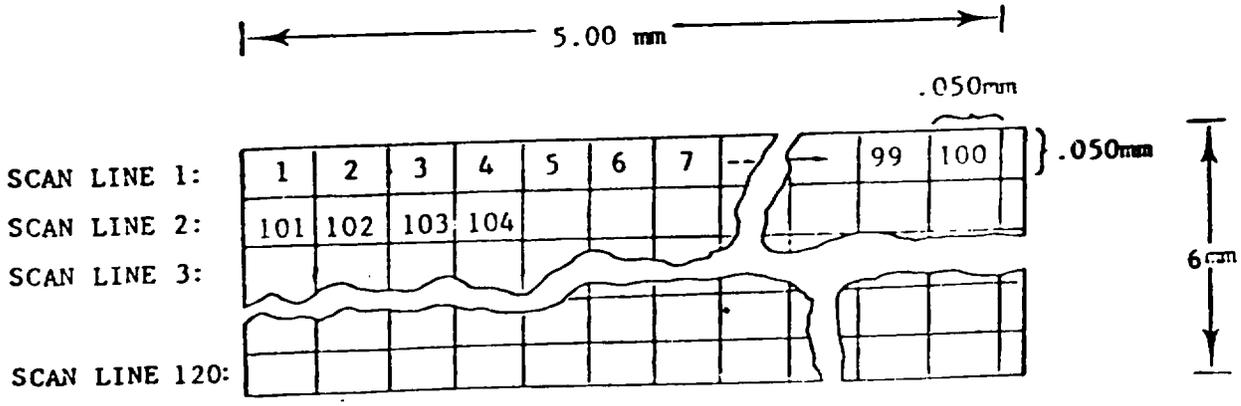

Figure 4-7. Microdensitometer Scan Sequence

microdensitometer and recorded in an input data set. A plot illustrating the average film response measured from the set is provided in Figure 4-8. By measuring the slope of the straight-line portion of each function, the average value of the film contrast was determined as $\gamma = 2.96$. This contrast, although not as high as had been determined in preliminary film tests at OTC, however, was sufficient for accurate evaluation of the smoke transmission.

The computer software, CONMAP, utilizes the film sensitometry data to relate the densities read from the smoke plume or sky background image to the relative scene brightness that produced each density. The code then compares the relative brightness values among the smoke image areas to an average relative brightness of the sky background to provide a ratio. The computer output for each pixel is a direct ratio indicating the smoke plume transmission:

$$\text{Transmission} = \frac{\text{Brightness of Smoke}}{\text{Brightness of Background}} \qquad (4\text{-}2)$$

An example transmission map is presented in Figure 4-9. Each symbol printed on the map represents a reading taken by the microdensitometer. Since the analysis is concerned only with smoke that appears darker than the sky background, areas that are brighter than or equal to the average background brightness are printed as blanks. The symbols, 0 through 9, indicate transmissions analyzed from the image of 88.8 percent to 93.8 percent. The symbols, A through J, are utilized to represent transmission of the plume from 93.8 percent to 98.9 percent. A "-" indicates areas where the transmission is less than 88.8 percent. The 98.8-percent upper limit results from the variability of the sky background brightness. In this case a one-standard deviation limit was placed on the average or mean background brightness to eliminate most of the fluctuations within the sky itself.

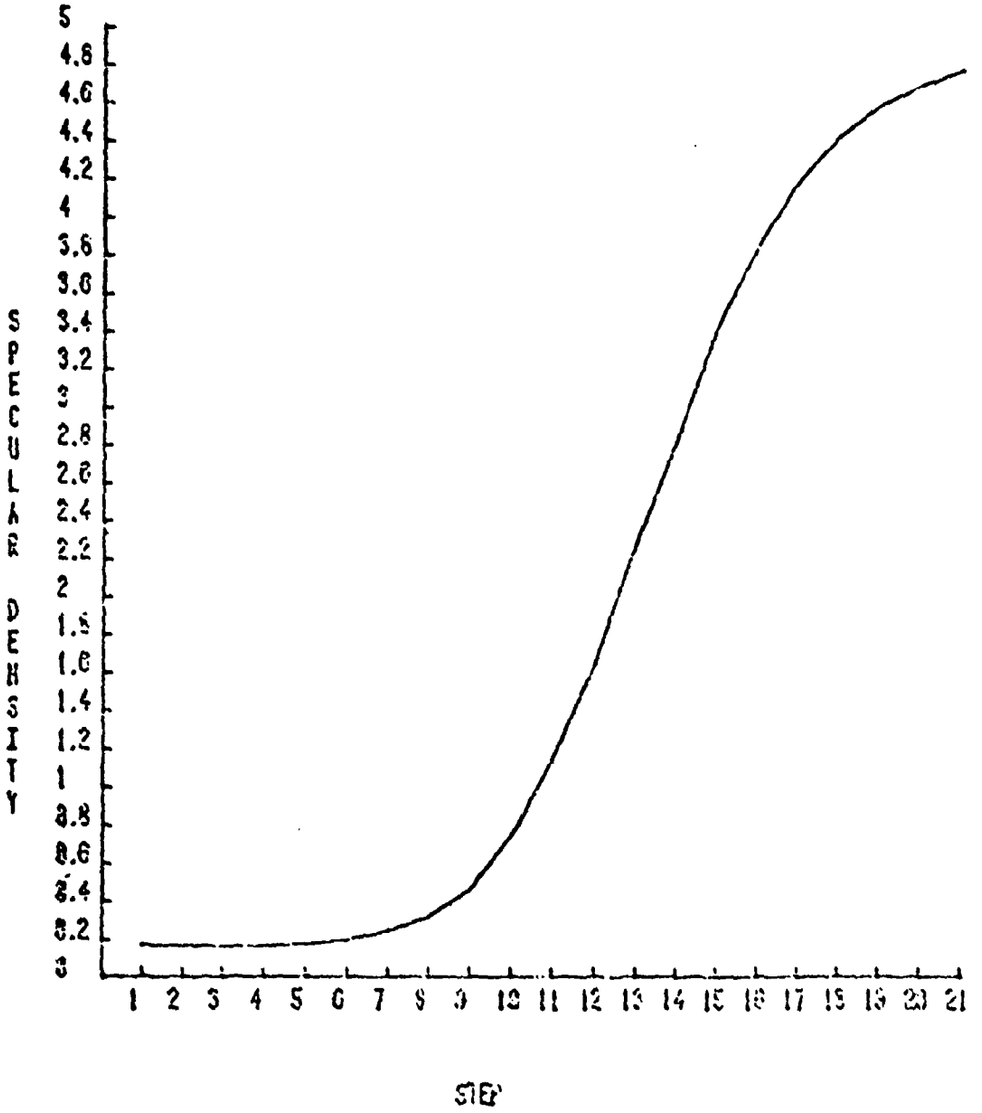

Figure 4-8. Technical Pan Characteristic Curve

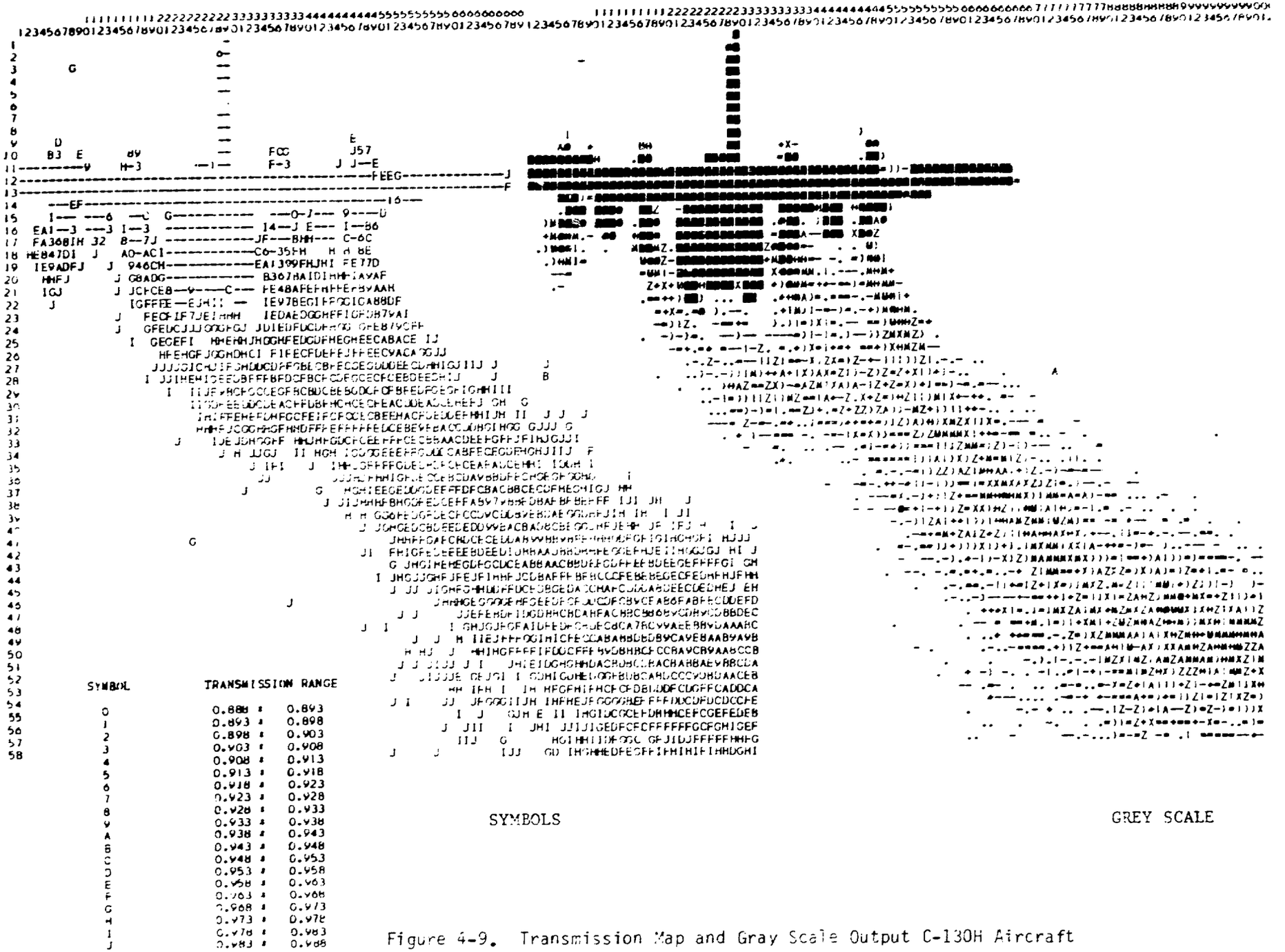

SYMBOL	TRANSMISSION RANGE	
0	0.888	0.893
1	0.893	0.898
2	0.898	0.903
3	0.903	0.908
4	0.908	0.913
5	0.913	0.918
6	0.918	0.923
7	0.923	0.928
8	0.928	0.933
9	0.933	0.938
A	0.938	0.943
B	0.943	0.948
C	0.948	0.953
D	0.953	0.958
E	0.958	0.963
F	0.963	0.968
G	0.968	0.973
H	0.973	0.978
I	0.978	0.983
J	0.983	0.988

SYMBOLS

GREY SCALE

Figure 4-9. Transmission Map and Gray Scale Output C-130H Aircraft

5. TEST RESULTS AND DISCUSSION

The program at Edwards FTC, planned to take 3 days, was completed in a single day of flight and ground testing. The professional conduct of the participants and the cooperation of their various organizations were responsible. Special credit is to be given to the flight crew of Aircraft 1586, Detachment 4, 2762nd Logistics Squadron, and the personnel of the 6510th Test Wing.

The objective of this program, which was to correlate engine ground test Smoke Numbers (Method SAE ARP 1179) with inflight exhaust trail visibility was accomplished. With this information, T56 engine Smoke Numbers can be specified to meet aircraft exhaust smoke visibility criteria. Secondarily, a conflict between DOD and EPA visibility specifications for turboprop engines could also be resolved.

5.1 FLIGHT TEST RESULTS

During the flight tests, various patterns were flown to simulate operations near and around airports, and to facilitate smoke observation and photography. The patterns were repeated with each fuel, then in part repeated again with the aircraft operating on both fuels. The two left engines were run on JP-4, and the two right ones on JP-5. Figure 5-1 shows the aircraft flying a parallel pass pattern during the testing. Tables 5-1, 5-2 and 5-3 summarize the flight patterns, engine conditions and meterological conditions of the test.

During the flight test period, scattered and broken clouds sometimes caused problems in making accurate transmission measurements. The clouds were documented at 20K ft to 25K ft altitude with coverage increasing from 10 percent to 70 percent during the tests. When the smoke plume is viewed against a nonuniform brightness sky or cloud background, the visual and

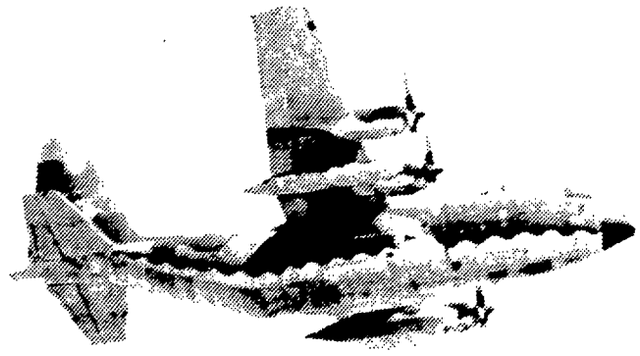

Figure 5-1. C-130H Flying Parallel Pass During T56 Exhaust Smoke Tests at Edwards FTC

TABLE 5-1. C-130H FLIGHT TEST DATA T56 SMOKE VISIBILITY AND DETECTION TEST EDWARDS FTC, 20 MAY 1980

Run No.	Time (Local)	Flight Pattern	Airspeed (Knots)	Altitude (Feet Above Terrain)	Aircraft Configuration	Fuel Used
1	.0830	Approach & Landing	--	T/D - 2000 Feet Marker	50% Flap	JP-4
2	.0841	Takeoff & Climb	--	L/O - 1500 Feet Marker	50% Flap	JP-4
3	.0844	Approach & Landing	--	T/D - 1500 Feet Marker	100% Flap	JP-4
4	.0850	Takeoff & Climb	104	L/O - 1500 Feet Marker	50% Flap	JP-4
5	.0853	Overhead Pass, Flight Idle Power	230 & DCR	300	Clean	JP-4
6	.0857	Overhead Pass, Approach Power	200	300	Clean	JP-4
7	.0901	Overhead Pass, Cruise Power	255	500	Clean	JP-4
8	.0905	Overhead Pass, Climb Power	290	500	Clean	JP-4
9	.0911	Overhead Pass, Takeoff Power	280	500	Clean	JP-4
10	.0916(1)	Parallel Pass, Flight Idle Power	180	500	Clean	JP-4
11	.0920	Parallel Pass, Flight Idle Power	200	400	Clean	JP-4
12	.0924	Parallel Pass, Approach Power	200	425	Clean	JP-4
13	.0928	Parallel Pass, Cruise Power	260	400	Clean	JP-4
14	.0933	Parallel Pass, Climb Power	275	500	Clean	JP-4
15	.0937	Parallel Pass, Takeoff Power	290	500	Clean	JP-4
16	.0942(2)	Overhead Pass, Flight Idle Power	180	400	Clean	JP-5
17	.0946	Parallel Pass, Flight Idle Power	230-180	500	Clean	JP-5
18	.0949	Parallel Pass, Approach Power	190	500	Clean	JP-5
19	.0952(1)	Parallel Pass, Cruise Power	240	500	Clean	JP-5
20	.0955	Parallel Pass, Cruise Power	255	400	Clean	JP-5
21	.0958	Parallel Pass, Climb Power	260-270	500	Clean	JP-5
22	.1001	Parallel Pass, Takeoff Power	280	450	Clean	JP-5
23	.1006	Approach & Landing	121	T/D - 2000 Feet Marker	100% Flap	JP-5
24	.1008	Takeoff & Climb	100	L/O - 2000 Feet Marker	50% Flap	JP-5
25	.1012	Approach & Landing	100	T/D - 2000 Feet Marker	100% Flap	Mixed(3)
26	.1014	Takeoff & Climb	100	L/O - 2000 Feet Marker	50% Flap	Mixed
27	.1017	Parallel Pass, Takeoff Power	290	500	Clean	Mixed
28	.1021	Parallel Pass, Takeoff Power	280	400	Clean	Mixed

NOTES:

(1) No Photo Data.
(2) Cloud Cover Problem, Deleted Overhead Pass.
(3) Left Engines JP-4, Right Engines JP-5.

TABLE 5-2. Engine Operating Conditions

Run No.	HORSEPOWER[1]				FUEL FLOW (LB/HR)				TORQUE (1000's of IN-LB)				TURBINE IN TEMP. (°F)			
	1	2	3	4	1	2	3	4	1	2	3	4	1	2	3	4
1	767	767	757	763	900	900	900	900	3.50	3.50	3.45	3.48	650	650	650	650
2	4111	4320	4100	4100	2100	2150	2150	2100	18.75	19.70	18.70	18.70	1076	1080	1071	1076
3	1096	1096	1096	1096	1000	1000	1000	1000	5.00	5.00	5.00	5.00	700	700	700	700
4	3311	3421	3278	3289	1000	1000	1050	1040	15.10	15.60	14.95	15.00	990	995	990	900
5	11	22	0	22	700	700	750	705	0.05	0.10	0.00	0.10	550	550	540	550
6	1316	1316	1316	1316	1075	1075	1075	1075	6.00	6.00	6.00	6.00	725	725	725	725
7	2566	2566	2566	2566	1500	1500	1500	1500	11.70	11.70	11.70	11.70	875	875	875	875
8	3815	3815	3815	3859	2000	2000	2000	2000	17.40	17.40	17.40	17.60	1010	1010	1010	1010
9	4298	4298	4298	4298	2200	2200	2200	2200	19.60	19.60	19.60	19.60	1060	1060	1065	1060
10	0	0	0	0	650	650	650	650	0.0	0.0	0.0	0.0	550	550	550	550
11	0	0	0	0	600	600	600	600	0.0	0.0	0.0	0.0	550	550	550	550
12	1316	1316	1316	1316	1100	1100	1100	1100	6.0	6.0	6.0	6.0	730	730	730	730
13	2500	2500	2500	2500	1500	1500	1500	1500	11.40	11.40	11.40	11.40	875	875	875	875
14	3837	3837	3837	3837	2000	2000	2000	2000	17.50	17.50	17.50	17.50	1010	1010	1010	1010
15	4298	4298	4298	4298	2100	2100	2100	2100	19.60	19.60	19.60	19.60	1060	1060	1060	1060
16	0	0	0	0	700	700	700	700	0.0	0.0	0.0	0.0	550	550	550	550
17	0	0	0	0	600	600	600	600	0.0	0.0	0.0	0.0	550	550	550	550
18	1360	1360	1360	1360	1100	1100	1100	1100	6.0	6.0	6.0	6.0	725	725	725	725
19	2587	2587	2587	2587	1600	1600	1600	1600	11.80	11.80	11.80	11.80	875	875	875	875
20	2587	2587	2587	2587	1600	1600	1600	1600	11.80	11.80	11.80	11.80	875	875	875	875
21	3728	3728	3728	3728	2000	2000	2000	2000	17.00	17.00	17.00	17.00	1010	1010	1010	1010
22	4298	4298	4298	4298	2150	2150	2100	2120	19.60	19.60	19.60	19.60	1065	1065	1065	1065
23	219	219	219	219	600	600	600	600	1.00	1.00	1.00	1.00	700	700	700	700
24	4298	4298	4298	4298	2000	2000	2000	2000	19.60	19.60	19.60	19.60	1065	1070	1070	1070
25	263	263	263	263	1000	1000	1000	1000	1.20	1.20	1.20	1.20	660	660	660	660
26	4298	4298	4298	4298	2100	2100	2100	2100	19.60	19.60	19.60	19.60[2]	1070	1075	1070	1070
27	4298	4298	4298	4298	2100	2100	2100	2100	19.60	19.60	19.60	19.60	1065	1065	1065	1065
28	4298	4298	4298	4298	2100	2100	2100	2100	19.60	19.60	19.60	19.60	19.60	1065	1065	1065

NOTES:

(1) Measured at Power Section, Gear Losses and Accessory Loads Not Substracted.

(2) Corrected from 17600 in. lb Based on TIT & Fuel Flow.

TABLE 5-3. Ambient Conditions EAFB Weather Station

Run No.	Time (Local)	Temperature (°F) (1)	Pressure (IN HG)	Humidity (LB/LB Dry Air)	Cloud Cover (Altitude & % Cover)	Wind Speed & Direction (MPH, True HDG)		Visibility (MI)
1	.0830	67	27.51(1)	.0071(1)	25,000 SCT, 10%	2	10	45
2		68	27.51	.0071				
3		69	27.51	.0071				
4		69	27.51	.0071				
5	.0853	70	27.515	.00713	25,000 SCT, 30%	0	0	35
6	.0857	70	27.52(1)	.00713				
7		71	27.52	.00713				
8		72	27.52	.00713				
9		72	27.52	.00713				
10		73	27.52	.00713				
10		73	27.52	.00713				
12		73	27.52	.00713				
13		74	27.51(1)	.00713				
14		74	27.51	.00713				
15		75	27.51	.00713				
16		75	27.51	.00713				
17		76	27.51	.00713				
18		76	27.51	.00713				
19		76	27.51	.00713				
20		77	27.510	.00713	20,000 SCT & 25,000 BKN ZOX	0	0	35
21		77	27.510	.00713				
22		77	27.510	.00713				
23		77	27.510	.0072(1)				
24		77	27.510	.0072				
25		78	27.510	.0072				
26		78	27.510	.0072				
27		78	27.510	.0073(1)				
28	.1021	78	27.510	.0073				

NOTES:

(1) Interpolated Between Readings at .0755, .0855, .0955 & .1055.

photographic methods of measuring the plume transmissions are hindered. Figure 5-2 illusrates this condition.

5.2 GROUND TESTS RESULTS

During the ground tests the inboard engines were operated at four power levels; Flight Idle, Approach, Cruise and Climb, and on the same fuel which was used during flight test. Takeoff power, which was originally planned, was not run to reduce the possibility of smoke line failure, or other difficulty due to the heavy buffeting of the aircraft which was encountered at climb power. Because of the T56 engine smoke characteristic, which is almost flat over the power range, this omission was judged not to detract from the validity of the test.

The JP-4 and JP-5 fuels, sampled from the aircraft tanks, were analyzed by the Fuels and Lubricants Laboratory at Wright Aeronautical Laboratories (AFWAL/POSF). The analyses, given in Table 5-4 show that the JP-4 fuel used was within specification. However, the JP-5 fuel had a smoke point of 17 mm which was 2 mm below specification. This characteristic would result in an exhaust plume which was smokier and more visible than an average JP-5, with a smoke point of 20.0 mm (Reference 32).

5.2.1 Smoke Tests

The Smoke Number (SN) which were obtained during the ground tests are given in Table 5-5, along with other pertinent engine data. The smoke signature of the engine was similar to that obtained during factory test stand measurements, of T56 engines. Figure 5-2 shows these smoke test results, plotted against measured engine horsepower. The engine exhaust SN for operation on JP-5 fuel averages 58, which is 10 SN higher than with JP-4. It should be noted that Smoke Numbers varied little with engine horsepower, especially in the range of 2000 hp or greater.

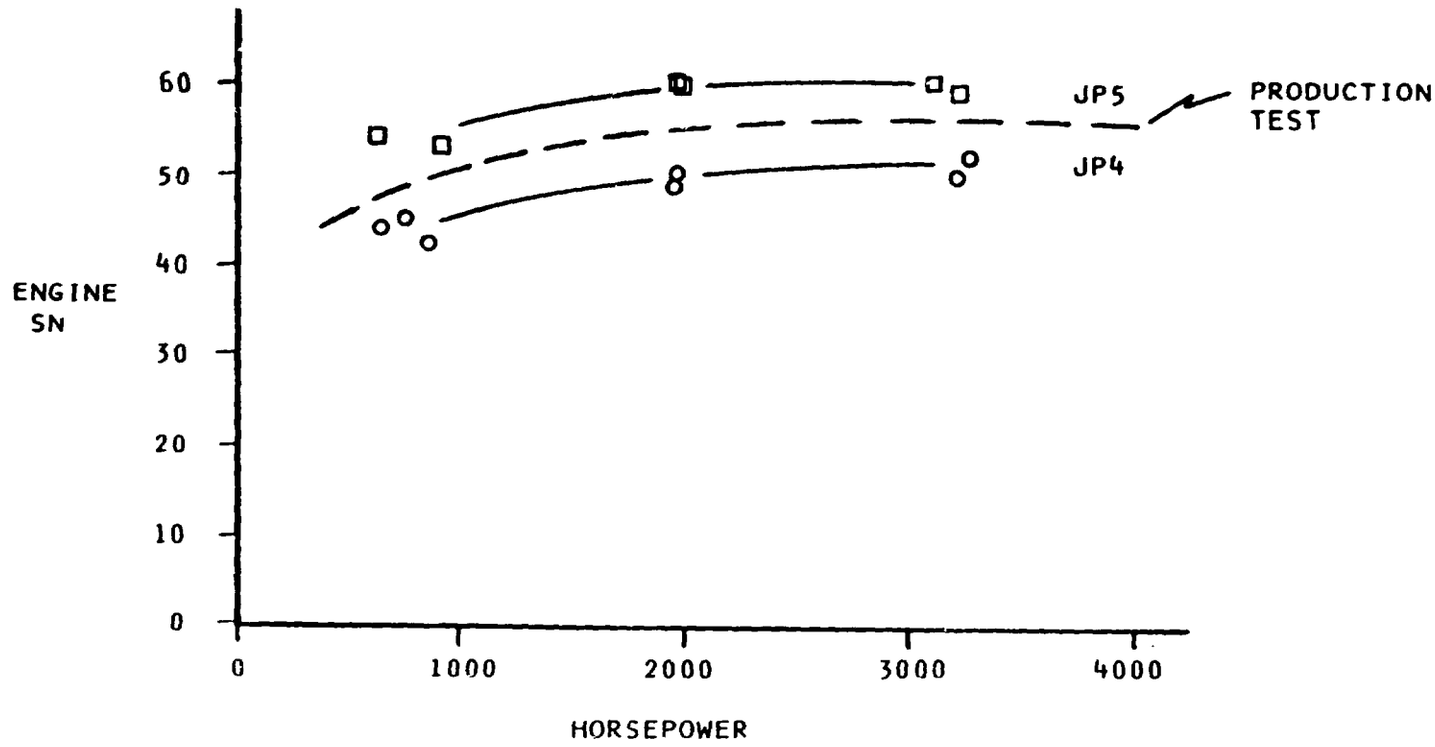

Figure 5-2. Smoke Test Results From Ground Test of Engine No. 2

TABLE 5-4. ANALYSIS OF FUEL USED IN PROGRAM

Item	JP-4	JP-5
Composition		
Aromatics, vol %	10.4	19.1
Olefins, vol %	0.8	0.4
Volatility		
Distillation iBP, °C	24	70
10%	67	173
20%	102	189
50%	160	216
90%	226	267
95%	241	267
FBP	286	301
Flash Pt, °C	-	29.4
Gravity, API. 15.6°C	57.4	40.0
Vapor Pressure, lb Reid	2.3	0.3
Fluidity		
Freezing Pt, °C	-70	-54
Combustion		
Net Heat, Btu/lb	18,706	18,506
Luminometer No.	72	47.2
Smoke Pt, mm	26.0	17.0
Hydrogen, NMR % wt	14.34	13.62

TABLE 5-5. Ground Run Smoke Test, Engine No. 2

Run No.	TOD (Local)	Fuel Type	Smoke No.	Engine Operating Data					Ambient Air Conditions			
				Condit	TIT (°C)	Torque (In Lb)	RPM (%)	Horsepower (Indicated)	Temp (°F)	Press. (In Hg)	Humidity (% Rel)	Spec. (lb/lb dry air)
1	.1352	JP4	44	Flt Idl	710	2800*	96	589	91.7	27.42	16	.0060
2	.1358	"	45	APR	725	3100	98	680	92.9	27.43	"	"
3	.1401	"	50	CRS	875	7900	100	1732	91.4	27.42	"	"
4	.1404	"	50	CLB	1010	13000	100	2851	92.7	27.42	"	"
5	.1407	"	49	CRS	875	8000	100	1754	93.2	27.42	"	"
6	.1411	"	52	CLB	1010	12400	100	2719	93.5	27.42	"	"
7	.1414	"	42	APR	730	3700	95	771	92.6	27.42	"	"
8	.1424	JP5	54	APR	725	2600*	95	542	92.6	27.41	"	"
9	.1426	"	60	CRS	75	8000	99	1737	91.9	27.42	"	"
10	.1428	"	59	CLB	1010	13000	100	2851	92.1	27.42	"	"
11	.1434	"	59	CRS	875	8000	100	1754	91.9	27.41	"	"
12	.1436	"	60	CLB	1010	12600	100	2763	93.3	27.41	"	"
13	.1439	"	53	APR	725	3800*	95	792	95.8	27.41	"	"

A/C C-130H, No. 73-1586
Eng T56-A-15, Ser No. AE106872

* Condition Lever at Flight Idle Stop

The fuel consumption values shown in Table 5-5 for "cruise" and "climb" power are considerably lower than the equivalent values obtained during flight testing. This is due to the constant speed of the T56 engine and to its control characteristics. In both cases the engines were governed to the same Turbine Inlet Temperature (TIT). However during flight, additional ram air was induced into the engines, and the engine control system scheduled more fuel to compensate and thusly hold TIT constant.

5.3 VISUAL OBSERVATIONS RESULTS

5.3.1 Ground Tests

The visual observations which were made during the ground runups are summarized in Table 5-6. The raw data can be found in the OEHL report, (Reference 33). Table 5-6 gives the average opacity readings, smoke numbers and the engine power for a given fuel type. It is evident from this data that Observer B's readings are consistently lower than those of Observer A on all test runs. This was confirmed by a standard statistical ("t" test). When the data were plotted graphically, it was found that the results are consistent from run to run, indicating a systematic error reading for one or both readers. More importantly, both observers were well within the range of observer differences expected for EPA Method 9 (Reference 33). According to Method 9 for black plumes, "99 percent of the sets were read with positive error of less than 5 percent." Thus, according to Method 9, as long as both observers read within 5 percent of each other, no true difference between readers existed. This emphasizes the weakness of visual observations made in accordance with Method 9 to discriminate between smoke plumes near the threshold of visibility.

Table 5-6 also shows lower opacity readings at climb power than at cruise power for JP-4. This dip was seen by both observers, neither of whom had knowledge of the engine settings until the data were tabulated. The reason for this is unknown. It is hypothesized that this may indicate that the

TABLE 5-6. VISUAL OBSERVATIONS GROUP RUN UP SUMMARY

Run	Opacity Average Observer A	Opacity Average Observer B	Engine Power Setting	Smoke No.	Fuel Flow lb/nr	Fuel
1	No Reading		flt idle	44	800	JP-4
2	4.4	1.1	approach	45	875	JP-4
3	5.8	3.3	cruise	50	1350	JP-4
4	5.0	3.7	climb	50	1700	JP-4
5	7.5	5.7	cruise	49	1360	JP-4
6	6.2	3.6	climb	52	1700	JP-4
7	5.5	3.3	approach	42	900	JP-4
8	5.8	5.0	approach	54	900	JP-5
9	9.2	8.4	cruise	60	1400	JP-5
10	10.0	7.1	climb	59	1800	JP-5
11	10.0	7.6	cruise	59	1400	JP-5
12	9.7	9.5	climb	60	1800	JP-5
13	7.1	5.3	approach	53	900	JP-5

engine produces different size particles at different power settings, and that these particles are more visible at cruise power. This observed result is more likely due to changes in smoke particle density in the propeller stream, which is at a higher velocity and turbulence at climb power than at cruise and hence would dilute the engine exhaust more. The T56 engine operates at constant mass flow over the power range. The increase in exhaust gas temperature from cruise to climb power would also contribute to this dilution effect.

5.3.2 Flight Tests

Opacity data from the visual observations made during the flight tests are summarized in Table 5-7. The raw data are available in the OEHL report

(Reference 34). Table 5-7 gives average opacity readings, engine power settings, engine fuel flow, and fuel type for each run made. Observer B's readings are presented for only that part of the flight path where readings were taken by Observer A. This portion is shown in Figure 4-1. It includes approach and flyby (Zones A-B and the beginning of the left turn past point B). Outside of this area, the exhaust plumes were never visible, that is, with an opacity of 2.6 percent or greater. The exhaust, therefore, did not add to the aircraft's visibility outside of the limited zones described in Table 5-7.

The results given in Table 5-7 indicate greater variability between observers during the flybys than for the ground runups. These differences may have resulted because of the distance between them. Certainly, the observation of a moving aircraft is more difficult than for a stationary source because of the constantly changing viewing angle to the plume. The morning sky also had considerably less contrast due to a diffuse cloud background at low viewing angles to the horizon. The variability between readers indicated serious problems in making quantitative inflight visual observations. The reduction in visible emissions between cruise and climb power noted during the ground runups for JP-4 also appears in the inflight data. Inflight opacity readings were below 21.4 percent in all cases.

Note that observations of a moving or stationary aircraft do not meet the definition of stationary source for EPA Method 9 -- Visual Determination of the Opacity of Emissions from Stationary Sources (Reference 33). The method requires that the observer stand:

- o at a distance from the plume sufficient to provide a clear view of the emissions;
- o with his line of vision approximately perpendicular to the plume direction; and
- o with the sun oriented in the quadrant to his back.

TABLE 5-7. VISUAL OBSERVATIONS, INFLIGHT SUMMARY

Run	Opacity Average ---Observer--- A	B	Engine Power Setting	Fuel Flow[1] lb/hr	Fuel
2	17.1	8.0	takeoff and climb	2125	JP-4
3	21.4	11.7	approach and land	1000	JP-4
4	16.0	6.0	takeoff and climb	1020	JP-4
5	15.8	6.0	flt idle	710	JP-4
6	15.4	8.0	approach	1075	JP-4
7	16.5	7.0	cruise	1500	JP-4
8	15.5	7.0	climb	2000	JP-4
9	18.8	5.0	takeoff (climb)	2200	JP-4
10	-	3.3	flt idle	650	JP-4
11	8.0	1.0	flt idle	600	JP-4
12	9.5	3.3	approach	1100	JP-4
13	12.5	5.0	cruise	1500	JP-4
14	11.0	4.2	climb	2000	JP-4
15	13.3	5.0	takeoff (climb)	2100	JP-4
16	-	6.0	abort/flt idle	700	JP-5
17	9.4	4.0	flt idle	600	JP-5
18	16.5	7.9	approach	1100	JP-5
19	-	7.0	cruise	1600	JP-5
20	18.5	7.0	cruise	1600	JP-5
21	18.9	6.0	climb	2000	JP-5
22	16.4	5.0	takeoff	2130	JP-5
23	20.8	8.3	approach and land	600	JP-5
24	14.2	10.0	takeoff	2000	JP-5
25	18.3/11/7	8.0	approach	1000	JP-5/JP-4
26	13.3/11/7	5.7	climb	2100	JP-5/JP-4
27	11.2[2]	4.2	takeoff	2100	JP-5/JP-4
28	10.0[2]	10.0	takeoff	2100	JP-5/JP-4

NOTES: [1]Fuel Flow is average of 4 readings, flight log.

[2]Opacity readings on one engine, but field notes do not specify if engine was using JP-4 or JP-5.

The method also requires that readings be made by observing the plume momentarily at 15-second intervals, over a 6-minute period, and at the point of greatest opacity. The average of these 24 readings is the observer evaluation of the plume.

5.3.3 Conclusions from Visual Observations

a. Stationary emissions standards are inappropriate for aircraft emission observations because of the difficulties in obtaining sufficient readings at one location for a valid series. Ringelmann readings (visual observations of opacity) can be prejudiced and hence somewhat subjective and inaccurate (Reference 35).

b. Although each observer was self-consistent in his own readings within the accepted variation (±5 percent opacity) the observer's readings were not consistent with each other during flight tests.

c. In-flight emissions were only visible during approach flybys and turn phases of the test. The emissions did not add to the aircraft visibility at any other time - this included flyby when the exhaust plume was perpendicular to the observer's line-of-sight.

d. Ground runup opacities did not exceed 10 percent with either JP-4 or JP-5 under any power condition.

e. In-flight opacity readings did not exceed 21 percent, even when the observer's line-of-sight nearly coincided with the exhaust plume path, an extremely conservative worst case.

f. The EPA's Smoke Number of 25-29 for a visible plume appears overly conservative. Smoke Numbers as high as 44 gave opacity readings as low as an average of 2.2 percent (JP-4 ground runup data, based only on visual observations).

5.4 PHOTOGRAPHIC/PHOTOMETRIC RESULTS

5.4.1 Flight Tests

Analysis of the imagery from Camera #2 provided smoke transmission data for the C-130 flight test sequences conducted at EAFB. As previously discussed, the film from Camera #1 was improperly exposed and could not be used to accurately determine the smoke plume transmission information.

The process of photometric data analysis is described in detail in Section 4.5 of this report. The processed photographs were analyzed to produce a map of digitized transmission data for each photograph which was taken. For illustrative purposes, symbols which appear to represent a progression from dark to light when printed can provide a simulated "photograph" of the scanned image when printed as a map, called a "grey-scale" map. Using this method, specific areas of the smoke plume that are of interest can be located. Grey scale maps are shown in Figures 5-5, 5-7, 5-9, 5-11 and 5-13.

The mean transmission of the smoke plume in each flight test photograph was determined using a statistical anlaysis routine, MAPSTAT. This code provides frequency distribution and mean values for a selected area of the transmission map bounded by a user specified polygon. An example output table produced by the MAPSTAT analysis of a smoke plume transmission map is shown in Figure 5-3. The table identifies the frequency of symbols on the map at each transmission level, the total number of pixels within the smoke plume, 1272, and the average plume transmission, 96.2 percent.

Because of the large quantity of data taken and anlayzed, only examples and not all of the transmission frequency distributions (normalized histograms) are provided in this report. A complete set of frequency distribution plots for all of the smoke test runs as well as a detailed description of all the photometry work in the program is provided in the report written by Scipar Inc., Buffalo, New York, (Reference 36).

FRAME A4-5

SYMBOL	TRANSMISSION RANGE	#
Ø	Ø.885 : Ø.89Ø	Ø
1	Ø.89Ø : Ø.895	Ø
2	Ø.895 : Ø.9ØØ	Ø
3	Ø.9ØØ : Ø.9Ø5	Ø
4	Ø.9Ø5 : Ø.91Ø	1
5	Ø.91Ø : Ø.915	1
6	Ø.915 : Ø.92Ø	1
7	Ø.92Ø : Ø.925	4
8	Ø.925 : Ø.93Ø	8
9	Ø.93Ø : Ø.935	19
A	Ø.935 : Ø.94Ø	29
B	Ø.94Ø : Ø.945	79
C	Ø.945 : Ø.95Ø	98
D	Ø.95Ø : Ø.955	129
E	Ø.955 : Ø.96Ø	168
F	Ø.96Ø : Ø.965	164
G	Ø.965 : Ø.97Ø	192
H	Ø.97Ø : Ø.975	115
I	Ø.975 : Ø.98Ø	144
J	Ø.98Ø : Ø.985	12Ø

**********MAP STATISTICS**********

NUMBER OF POINTS GREATER THAN Ø.885: 25
NUMBER OF POINTS BETWEEN LIMITS: 1272 ←
NUMBER OF POINTS LESS THAN Ø.985: Ø
NUMBER OF POINTS EQUAL TO THE BACKGROUND : 826

TRANSMISSION MEAN Ø.9622 ←
TRANSMISSION STD DEV Ø.Ø133

TRANSMISSION LINE-BY-LINE STATISTICS

LINE	DATA	MEAN	STD DEV
2Ø	25	Ø.9545	Ø.Ø2Ø7
21	29	Ø.9558	Ø.Ø171
22	29	Ø.9622	Ø.Ø162
23	32	Ø.9617	Ø.Ø155
24	33	Ø.9617	Ø.Ø134
25	37	Ø.9667	Ø.Ø111
26	36	Ø.9636	Ø.Ø122
27	41	Ø.9655	Ø.Ø114
28	4Ø	Ø.9613	Ø.Ø117
29	42	Ø.9611	Ø.Ø121
3Ø	42	Ø.9606	Ø.Ø114
31	42	Ø.9640	Ø.Ø119
32	43	Ø.9628	Ø.Ø1Ø2
33	41	Ø.9627	Ø.Ø119
34	36	Ø.9654	Ø.Ø119
35	33	Ø.9643	Ø.Ø115
36	29	Ø.9613	Ø.Ø122
37	32	Ø.9608	Ø.Ø1ØØ
38	32	Ø.9573	Ø.Ø148
39	31	Ø.9556	Ø.Ø144
4Ø	28	Ø.9538	Ø.Ø112
41	23	Ø.9546	Ø.Ø126
42	32	Ø.9591	Ø.Ø111
43	31	Ø.9596	Ø.Ø132
44	33	Ø.9668	Ø.Ø126
45	31	Ø.9625	Ø.Ø12Ø
46	3Ø	Ø.9637	Ø.Ø117
47	27	Ø.9551	Ø.Ø142
48	29	Ø.9573	Ø.Ø152
49	3Ø	Ø.96Ø7	Ø.Ø145
5Ø	31	Ø.96Ø7	Ø.Ø143
51	3Ø	Ø.9625	Ø.Ø134
52	31	Ø.9623	Ø.Ø131
53	31	Ø.9662	Ø.Ø111
54	32	Ø.9673	Ø.ØØ9Ø
55	29	Ø.9688	Ø.Ø111
56	27	Ø.9692	Ø.Ø1Ø5
57	28	Ø.9721	Ø.ØØ94
58	29	Ø.9722	Ø.ØØ8Ø

Figure 5-3. Statistical Output Tables from MAPSTAT

In the example given herein, the data are organized to present the transmission data from each photograph during a single flyby on one chart. The distrubution data were normalized to provide the relative frequency of each transmission value within the smoke plume.

Example 1 - Run No. 5

Run #5 was an overhead pass at idle power on JP-4 fuel.

Figure 5-4 illustrates the frequency distributions derived from Frames 2, 3, and 4 on Run #5. As the frame number increases, the observer's line-of-sight changes from being hearly parallel to the exhaust plume path to becoming more and more perpendicular. The distribution of transmission values for Frames 2 and 3 are very similar. For Frame 4, the overall average plume transmission measure between 97.5 percent and 98.5 percent within a single cell or bin, and, therefore, the distribution appears as a single line approaching 1.0 or 100 percent.

A grey scale map series of Run #5 is provided in Figure 5-5. The grey level in each map corresponds to various smoke transmission levels as indicated by the calibrated scale on the left side of the figure. The white areas of the map indicate areas of 98.5 percent transmission or higher.

Example 2 - Run No. 6

Run No. 6 was an overhead pass at approach power on JP-4 fuel.

The frequency distributions for the smoke transmission from Run #6 are shown in Figure 5-6. A grey scale map sequence for this run is provided in Figure 5-7. The average transmissison of the plume during this run ranges from 96 percent to 97.6 percent with portions of the plume at 89 percent transmission. As illustrated by the grey scale maps, the definition of a single plume is difficult because of the inconsistent accumulation of smoke

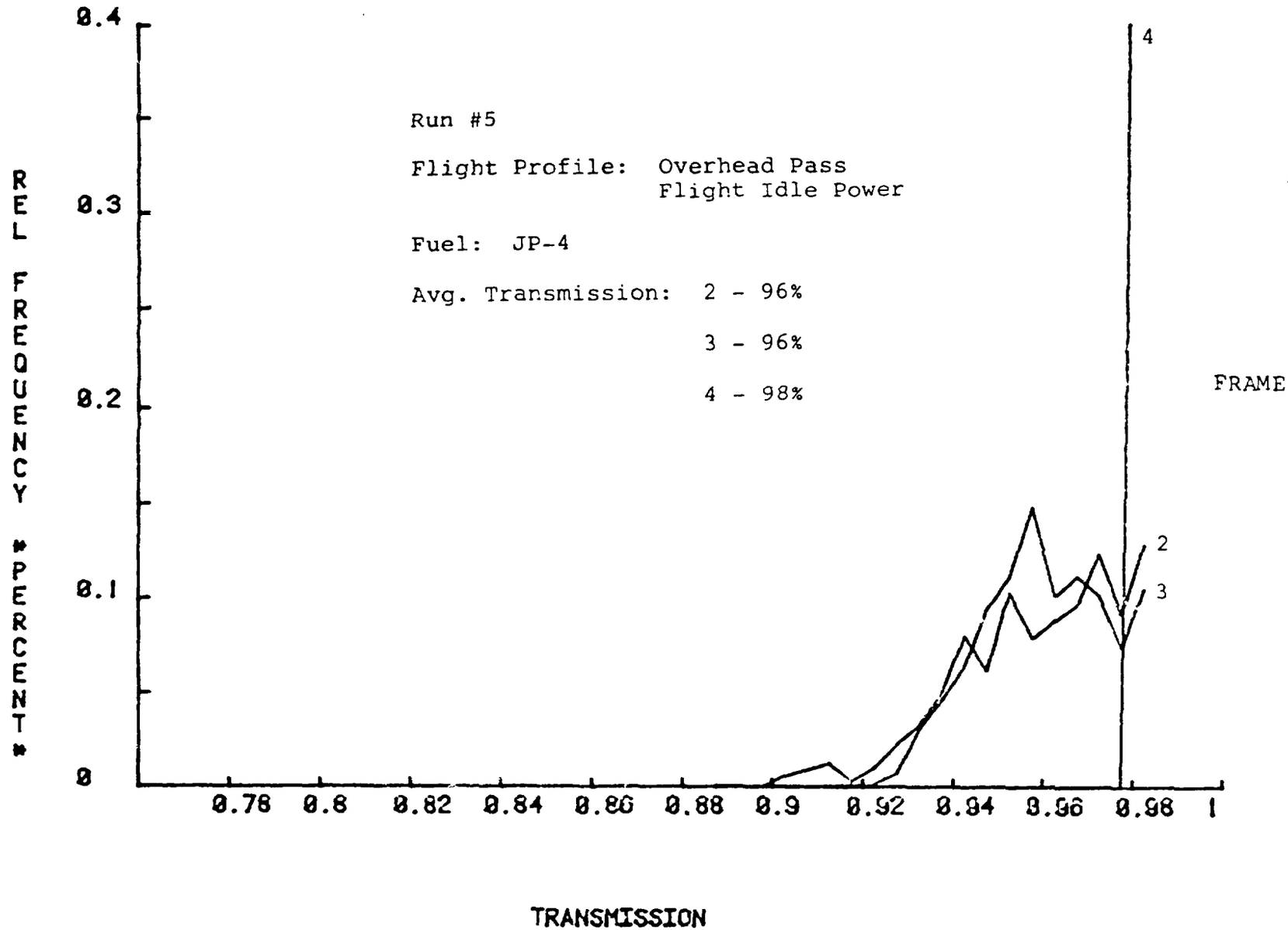

Figure 5-4 Relative Transmission Distribution - Run #5

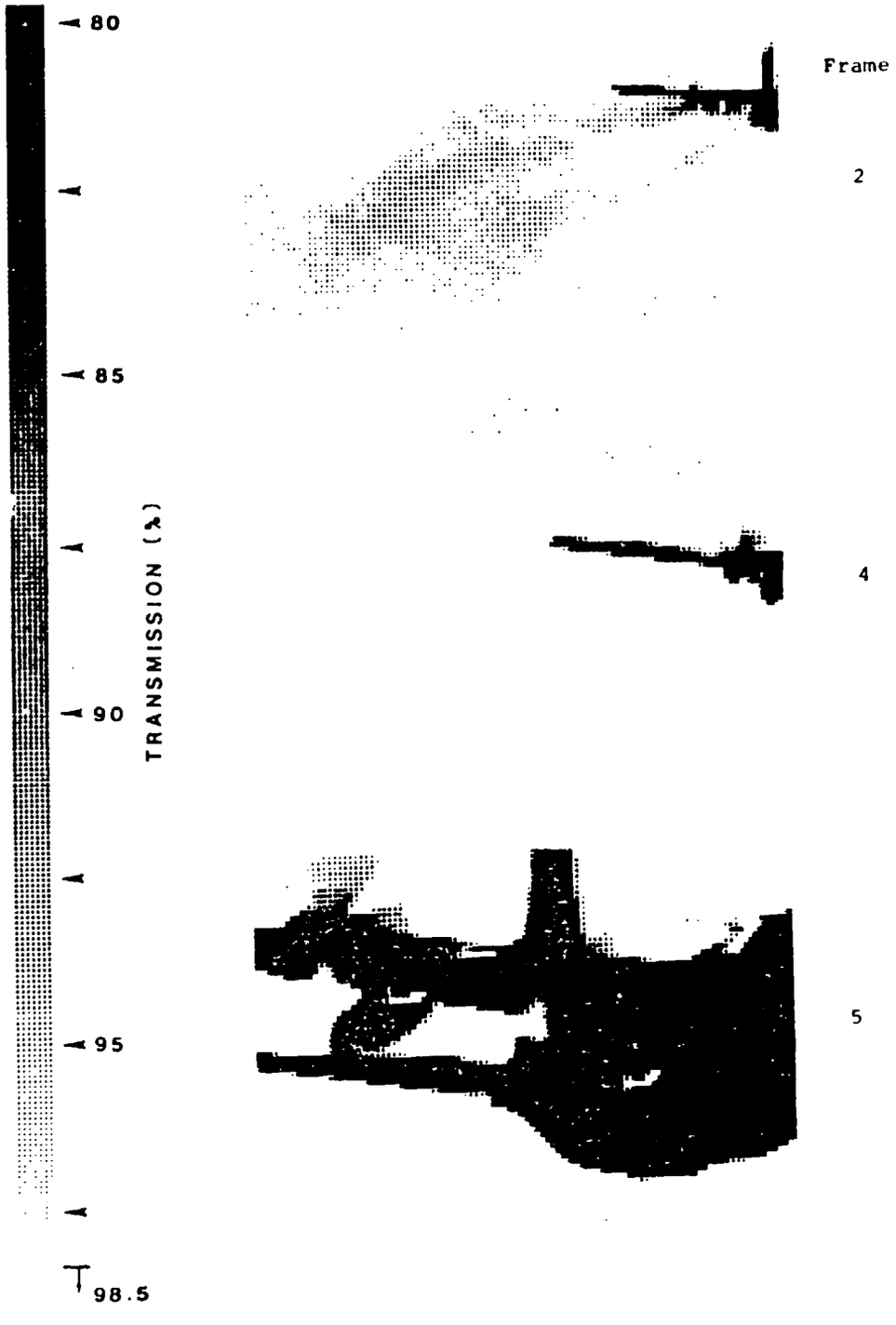

Figure 5-5. Grey Scale Maps - Run Number 5

Run #6

Flight Profile: Overhead Pass
Approach Power

Fuel: JP-4

Avg. Transmission: 1 - 96.6%
2 - 96.4%
3 - 96%
4 - 97.7%
5 - 97.6%

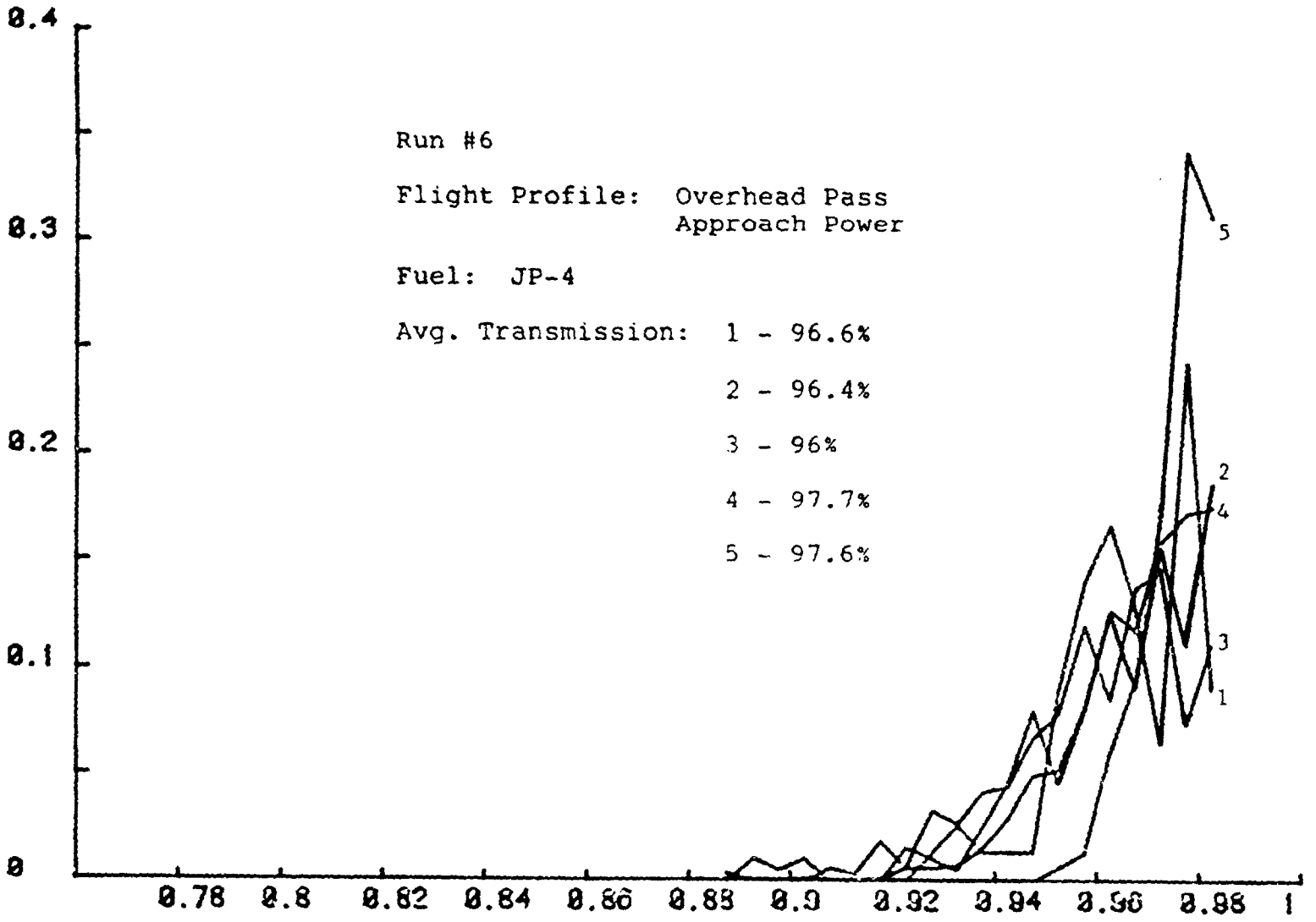

Figure 5-6. Relative Transmission Distribution - Run #6

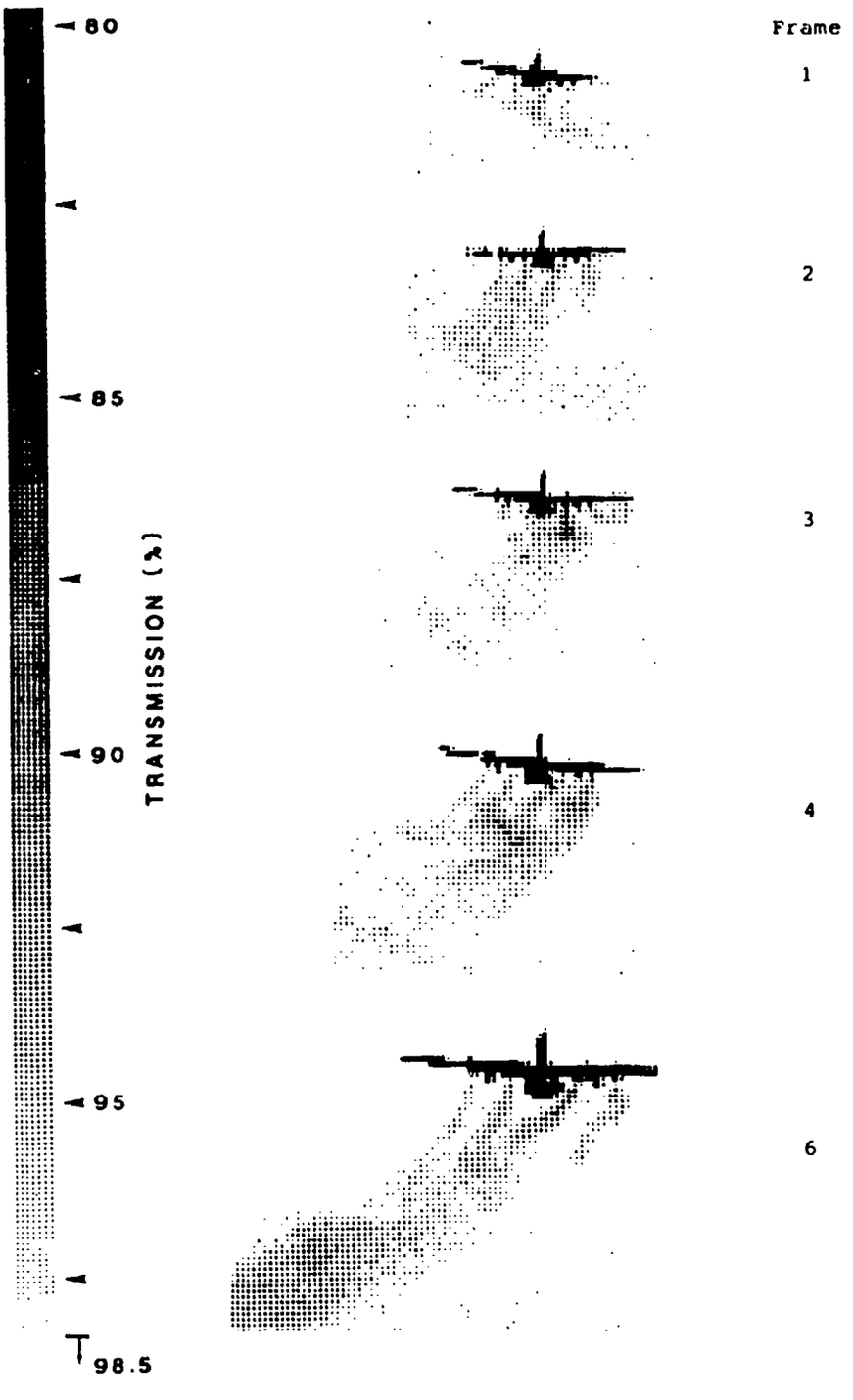

Figure 5-7 Grey Scale Maps - Run Number 6

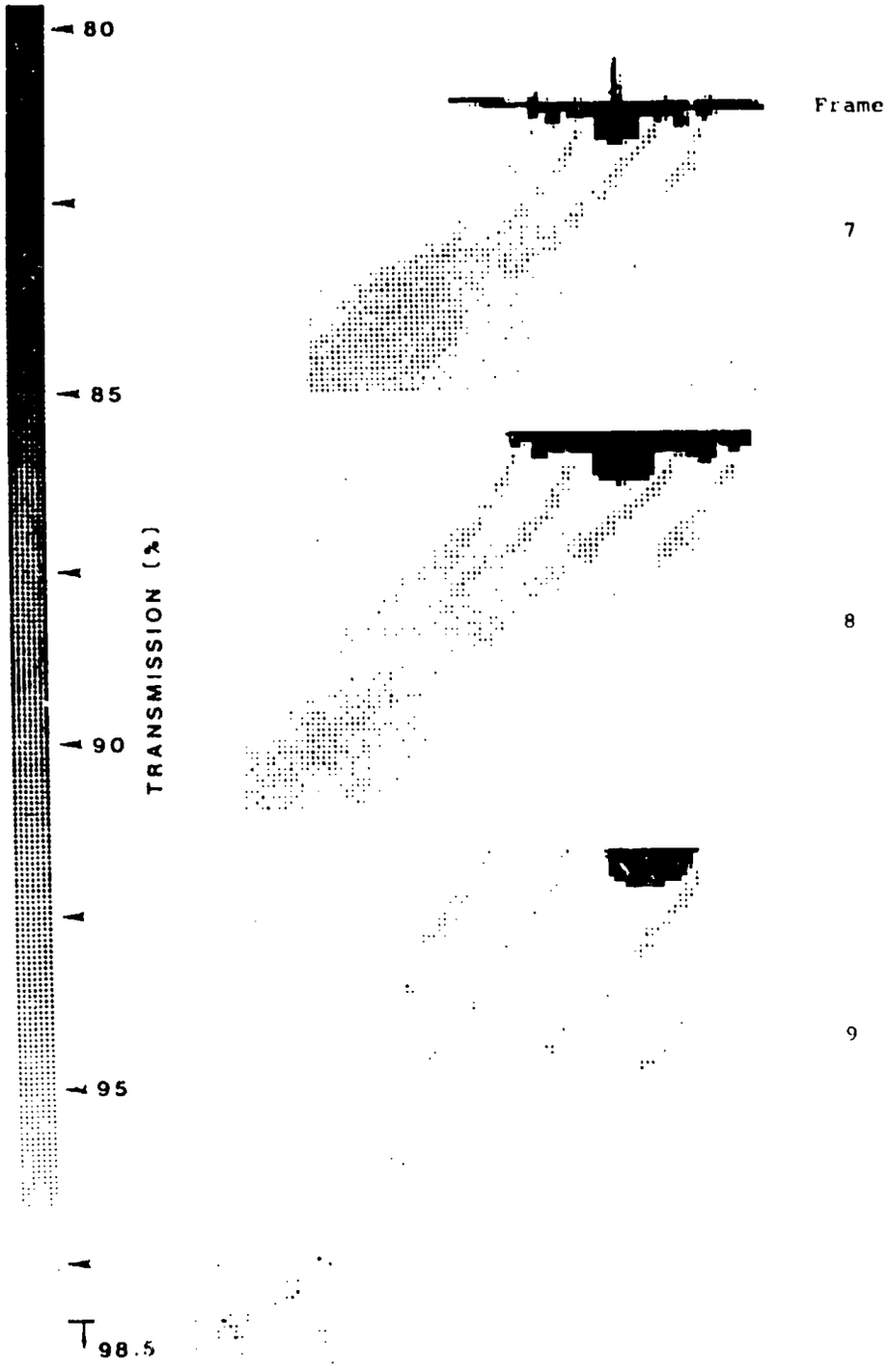

Figure 5-7 Grey Scale Maps - Run Number 6 (Concluded)

from each engine. The overall plume is generated by 3 to 4 engines in this sequence, however, the contribution of smoke from each engine is shown to vary. Note, however, that the transmission approaches 98 percent or greater in frame 9 as the line of observation is approaching a right angle with the exhaust plume.

Example 3 - Run No. 9

The smoke produced by the C-130 aircraft during Run #9 (Overhead pass, Takeoff power, JP-4 fuel) is plotted in Figure 5-8. The average plume transmission in Frame #3 was calculated as 95.6 percent, whereas the smoke in other frames from the run average above 97 percent. The distribution of transmission values throughout the plume is varied for each frame, however, Frame #3 illustrates that either the smoke production was increased (i.e., throttle change) or the dispersion of smoke was altered by atmospheric conditions. This is illustrated in the grey scale map sequence in Figure 5-9. Examination of the smoke in Frame #3 and Frame #4 shows the development of a dense smoke patch "moving away" from the aircraft. Note again that as the sequence increases, the higher viewing aspect angles (less plume depth) cause the transmission of the plume to approach 100 percent.

Example 4 - Run No. 13

The transmission data from Run No. 13 (Parallel pass, Cruise power, JP-4 fuel) is plotted in Figure 5-10 and mapped in Figure 5-11. This is an example of a run where the measured smoke was minimal. Transmission averages of 97.8 percent and 97.9 percent for Frames 5 and 6 were found, with no measurable smoke in Frame 7 and 8. The background "noise" illustrated at the top of Frame #8 results from variation in the background brightness within the frame. While the background is measured at these areas within the frame, only the average value is used in reducing the data. This method does not account for systematic variations in the background level. A more sophisticated algorithm could be developed that would include the systematic sky background

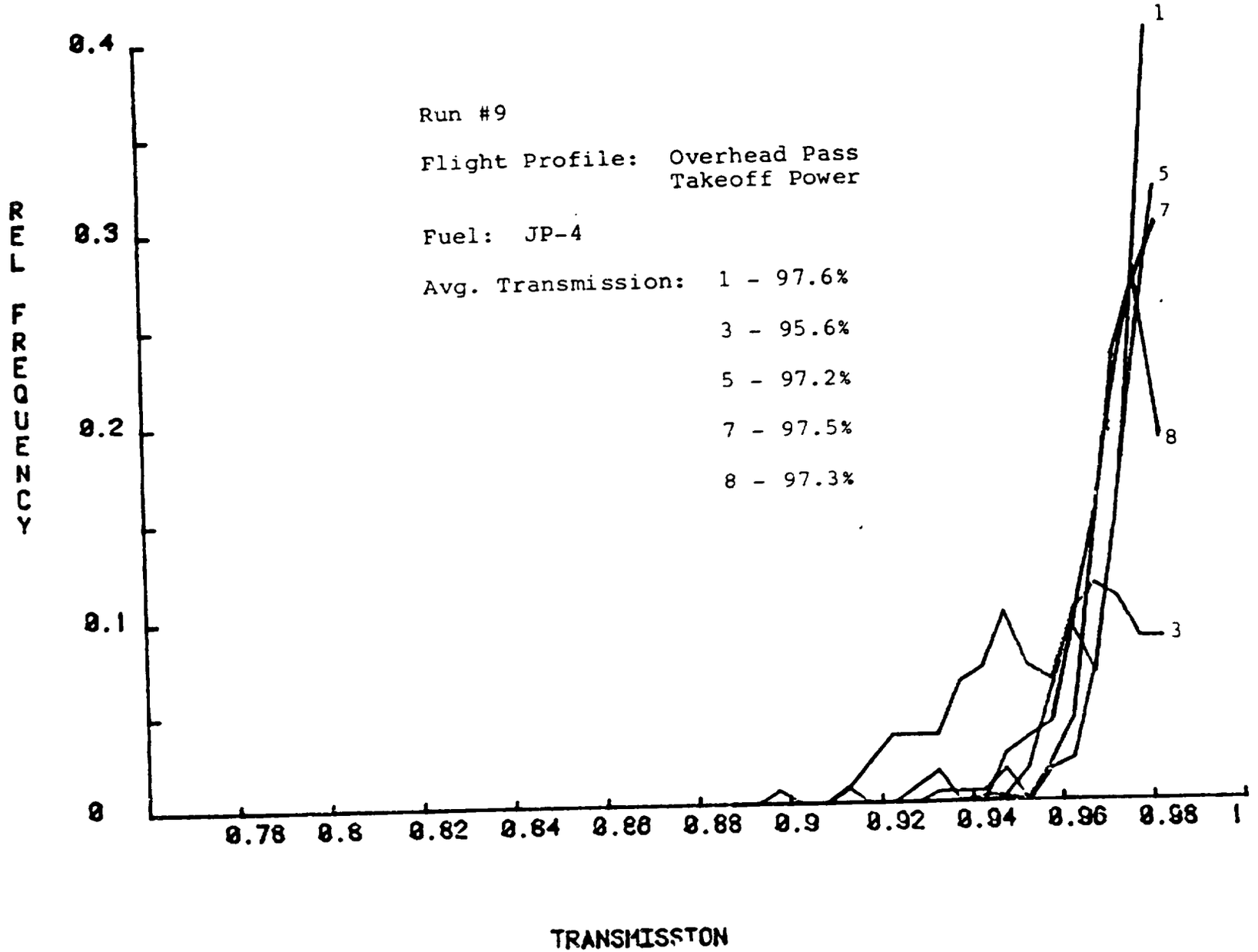

Figure 5-8 Relative Transmission Distribution - Run #9

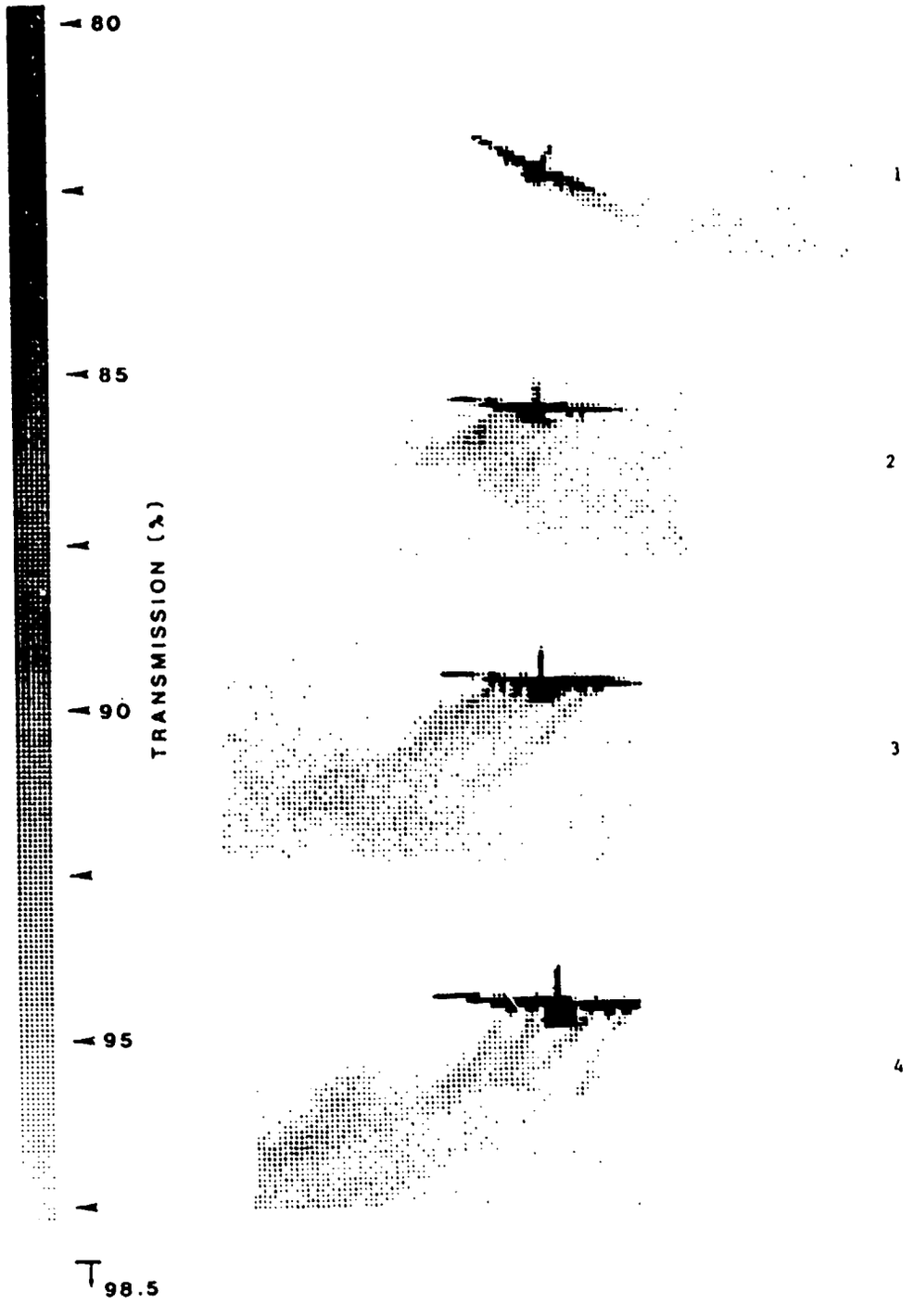

Figure 5.9 Grey Scale Maps - Run Number 9

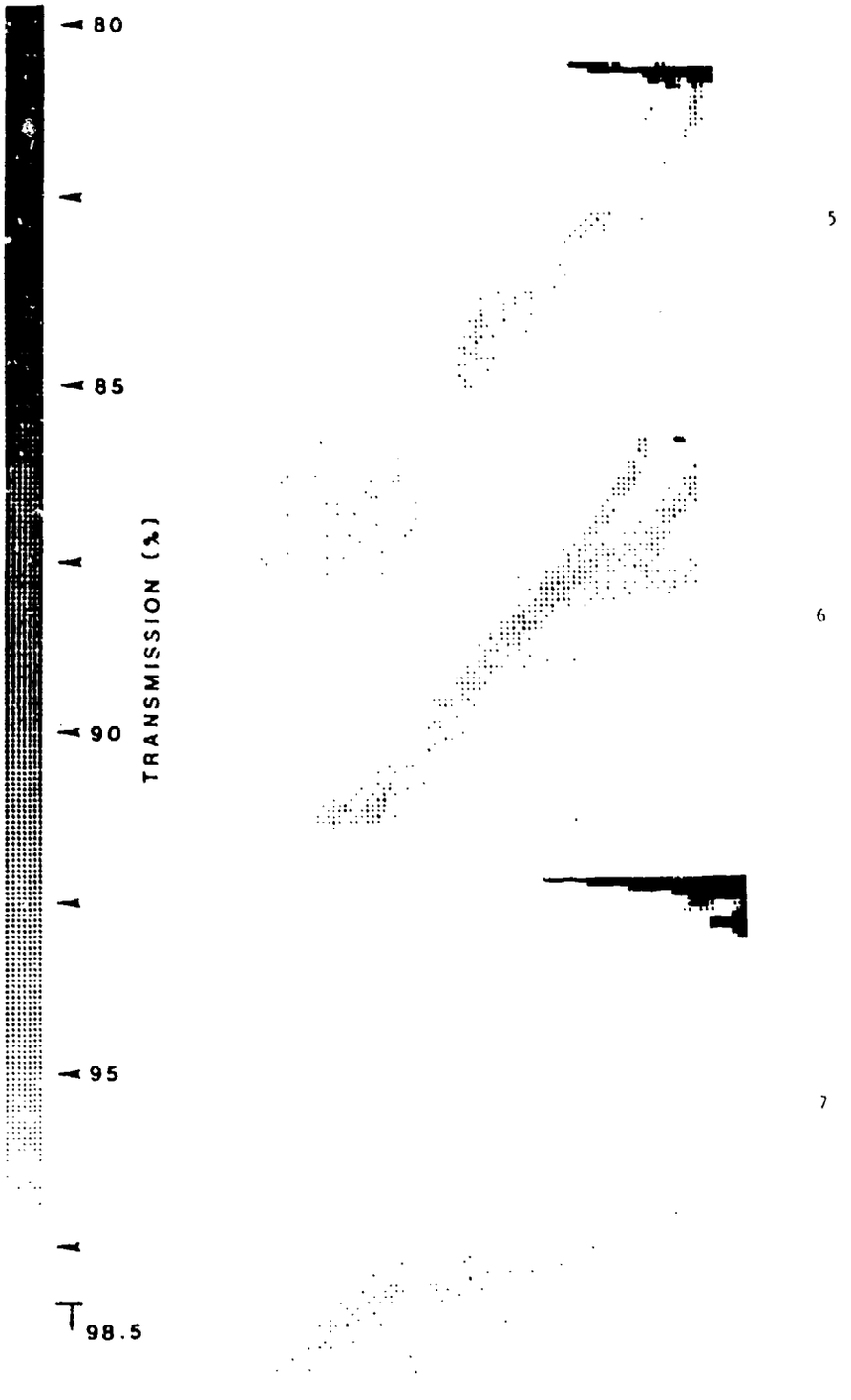

Figure 5.9 Grey Scale Maps - Run Number 9 (Concluded)

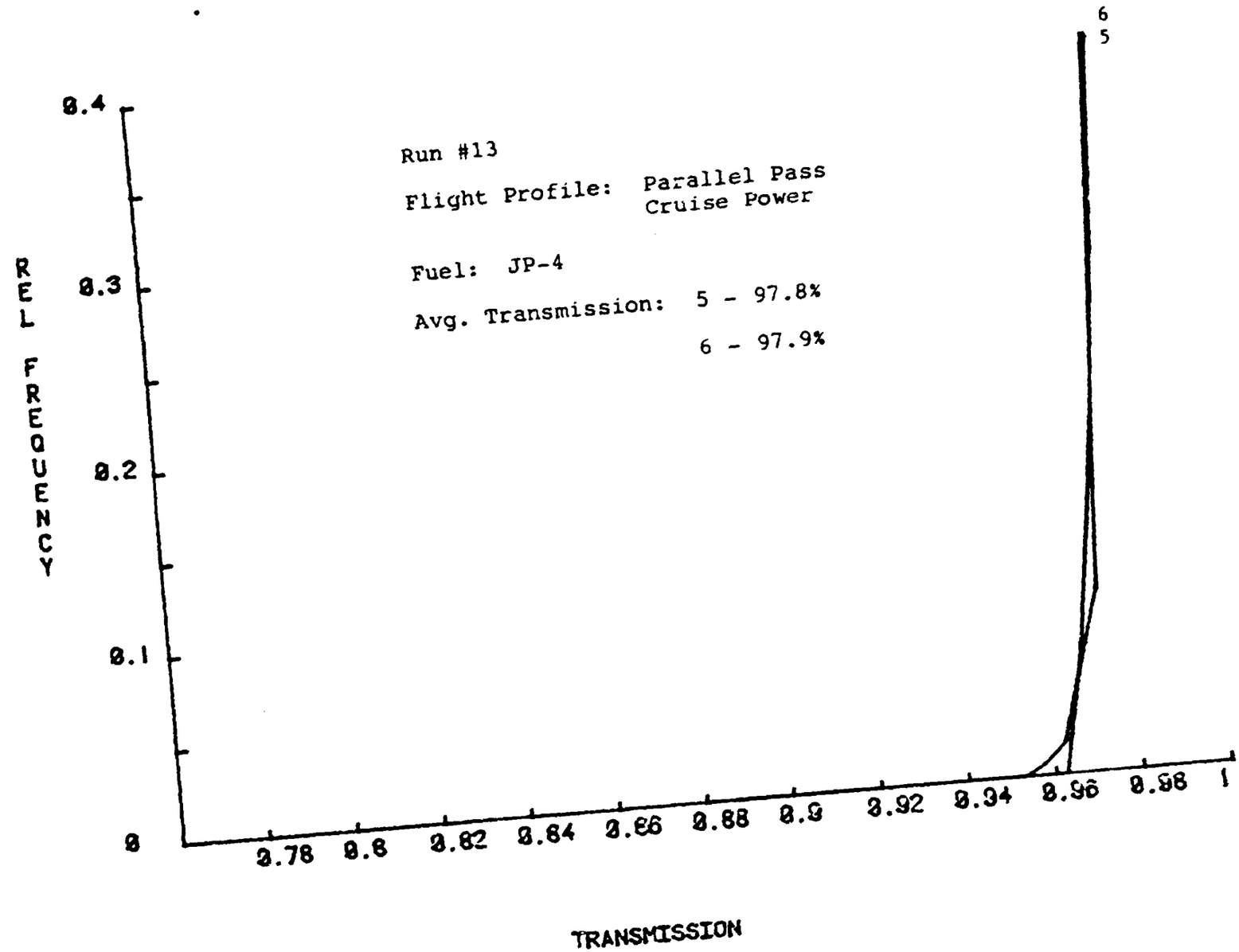

Figure 5-10 Relative Transmission Distribution - Run #13

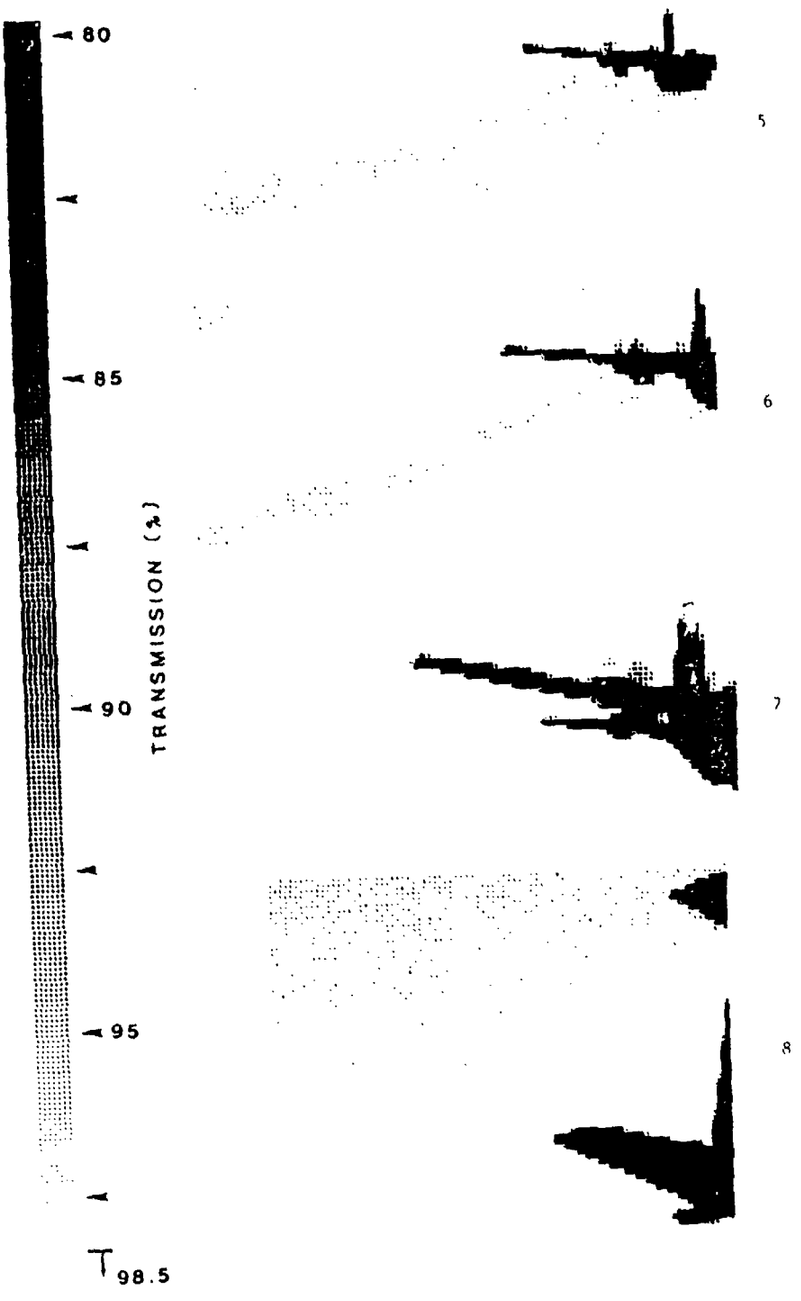

Figure 5-11 Grey Scale Maps -Run Number 13

variation, however, this is only a significant problem when the target is at a close range to the measurement camera or a large variation in background level is present for other reasons.

Example 5 - Run No. 15

The next example is Run #15 (Parallel pass, Takeoff power, JP-4 fuel). The relative frequency plot of smoke transmission is provided in Figure 5-12 and the grey scale maps in Figure 5-13. In Frame #1, the smoke is blocked by the aircraft and; therefore, no transmission data were available. Dark plume transmission values found in Frame #2 were due to the axial plume viewing aspect. As the sequence progressed, the viewing approached a perpendicular aspect and no smoke could be measured.

5.4.2 Ground Tests

Photographic data were collected during ground test to determine the plume transmission from a perpendicular aspect and relate these values to Smoke Number readings from a smoke meter. The collection of valid photographic information, however, requires a uniform brightness sky background. Transmission data could not be generated from the photographs, since the sky background viewed through the plume near the horizon was cloudy and non-uniform. The nonuniform background varied within the field-of-view of the camera enough that differences in measured brightnesses caused by the smoke could not be distinguished from background changes.

Successful readings of opacity by the observers, Smoke Numbers and the engine power for each test run were documented. The observers were able to evaluate the plume opacity (with some difficulty) by viewing a selected area and observing the brightness change due to the turbulent plume. By continuous observation of the plume, much more information was available to the observers than to the film for single instances.

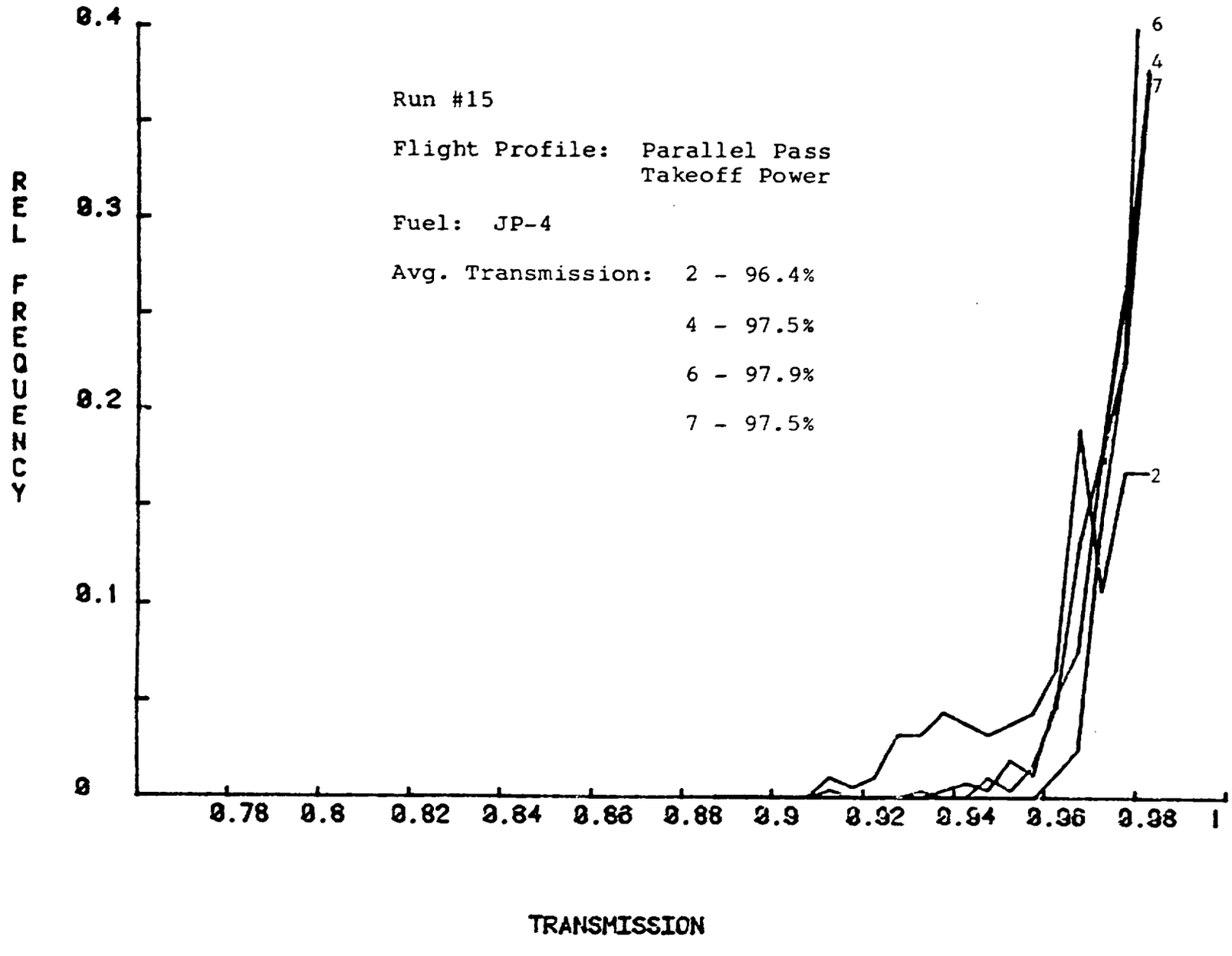

Figure 5-12 Relative Transmission Distribution - Run #15

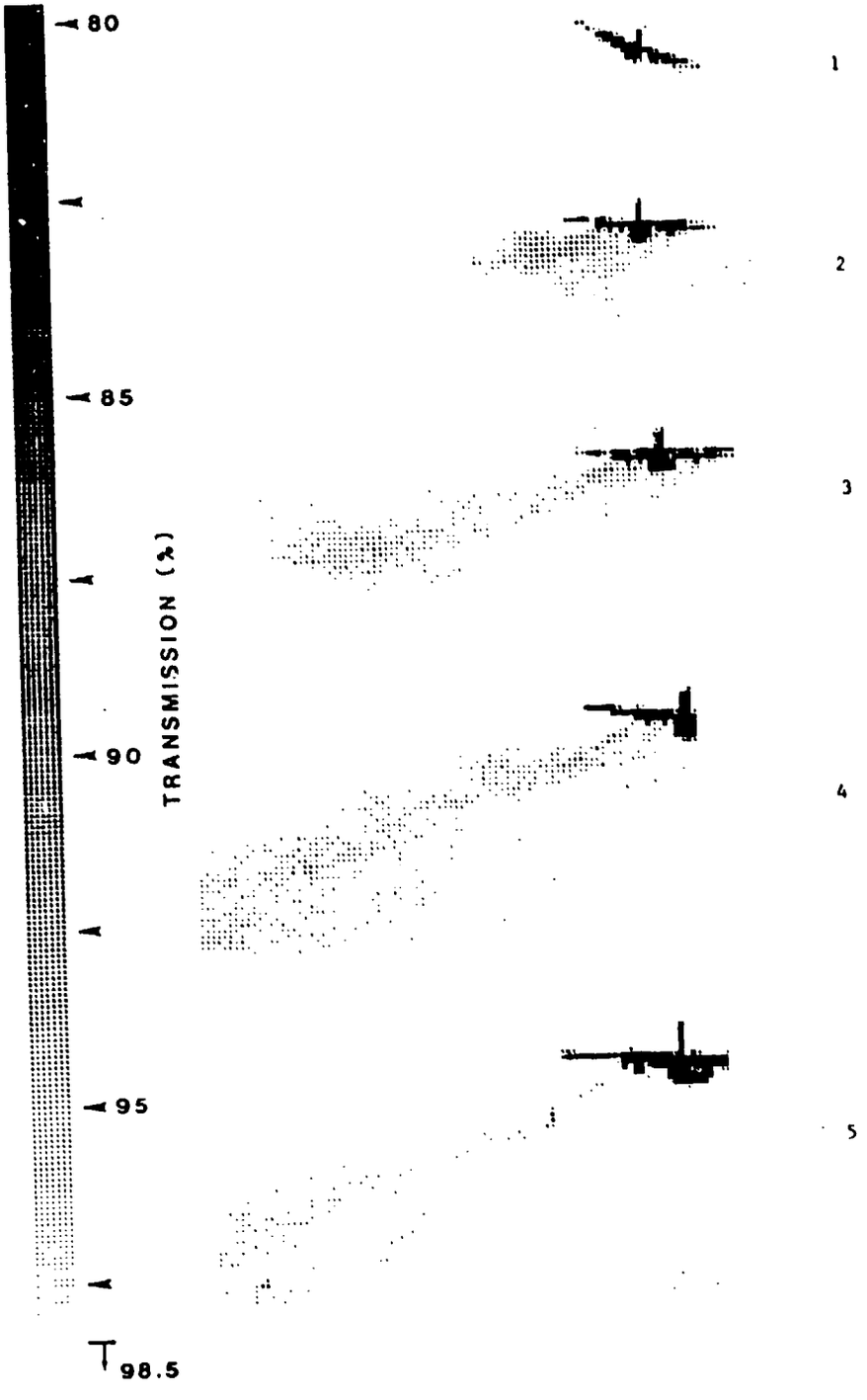

Figure 5-13 Grey Scale Maps - Run Number 15

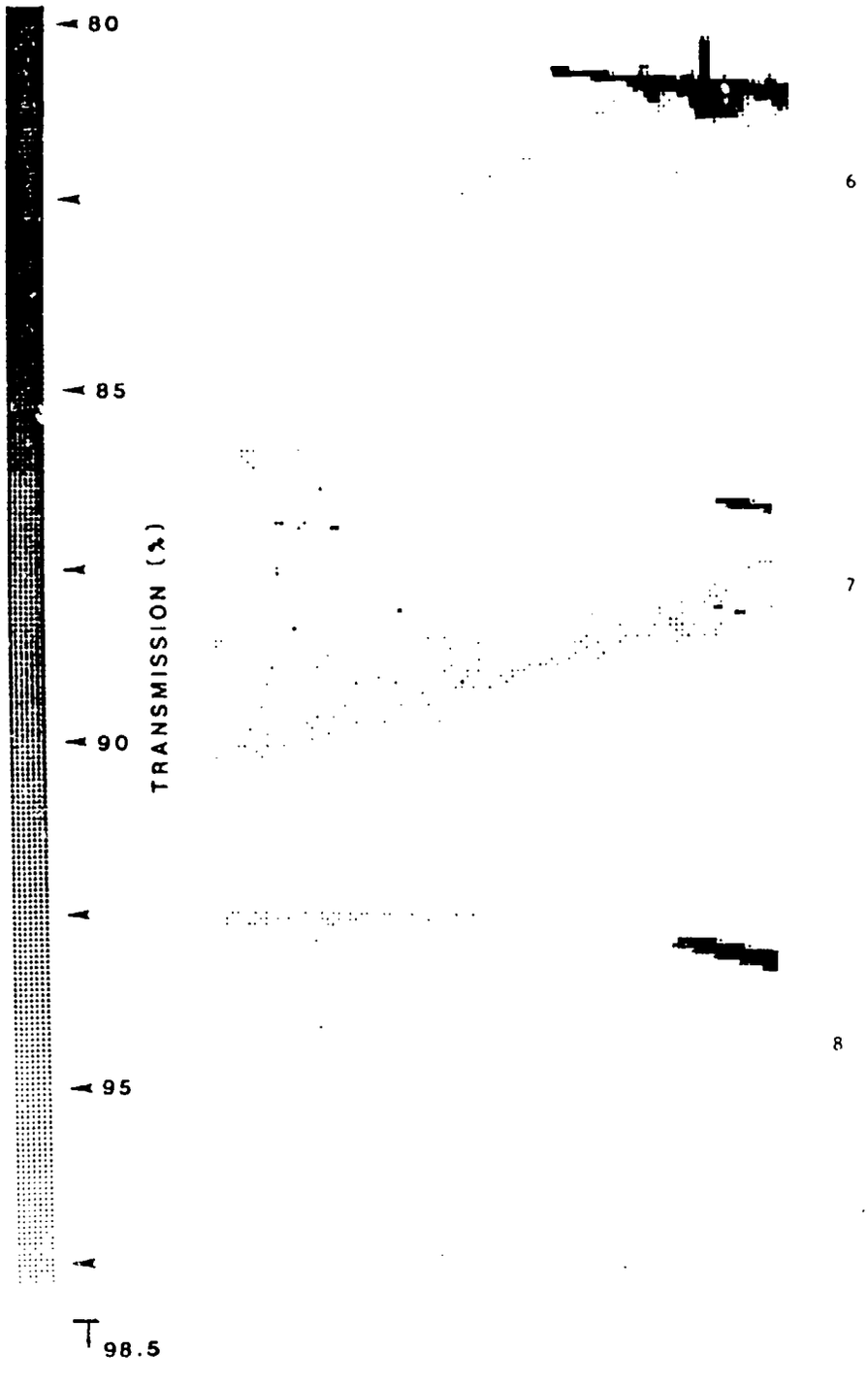

Figure 5-13 Grey Scale Maps - Run Number 15 (Concluded)

5.4.3 Conclusions from Photometric Testing

a. Average exhaust plume transmission values from 91.5 percent to over 98 percent were recorded during the testing encompassing a range of plume visibility from visible through invisible, as required in the program plan.

b. At all power levels the exhaust plumes approached 98 percent or greater (were invisible) when measured normal to the plume.

c. The variability of the background brightness prohibited the collection of valid photometric data during ground testing.

d. In some instances cloud formation during the flight testing inhibited making accurate transmission values. The grey scale maps showed this condition and provided for acceptable interpretation of the data which exhibited this type of noise.

5.5 TRANSMISSION MEASUREMENT COMPARISONS

The smoke plume data collected photographically are compared to the data documented by the two certified visual emission readers in this section. This involved examination of the darkest areas of the plume rather than the overall average, since on each run the observers attempted to view the darkest area of the plume and record its opacity (100-percent Transmission). A problem, in representing this visual estimation procedure in the analysis of the photographic data occurs in selecting the plume size comparable with that the observer views for generation of data. The angular resolution of the eye is approximately 1/60 degree (1 arc minute); however, the evaluation of opacity by the eye would not be made over that small an area. More realistically, it was assumed that the observers averaged over an angular area of 5 to 15 arc minutes in the darkest part of the plume.

The resolution of the grey scale maps is similar to that of the eye in that each pixel is a square with 1.72 arc minute sides. To reduce the photographic data to a value representing the darkest visual area, a standard data analysis format was developed. First, it was determined that the area of 26 pixels from the map equals the area of a circle with an angular diameter of 10 arc minutes. The next step was to represent the plume transmission data from each frame as a cumulative distribution. The data from Run #6 are plotted in Figure 5-14 for illustration. This plot illustrates the relative contribution of each transmission value to the overall smoke plume by examination of the slope of the curve. From this plot, the transmission value at 10 arc minutes size or after 26 pixels was found for comparison to the visual observer data. This value approximates the average transmission of the plume over a 5-to 15-arc minute size area. The cumulative frequency level corresponding to 26 pixels varies between frames since the size (total number of pixels) of the plume varies. The transmission values at 10 arc minutes are identified on each cumulative plot in Figure 5-14.

Comparison of the photographic and observer transmission data was accomplished by plotting the transmission values as a function of time. The transmission values from the observers were obtained from the opacity values that were documented in the OEHL Report. Figure 5-15 provides an example for Runs #6 and #7. (The remaining plots are supplied in Appendix D of the Scipar report.) The thin solid line represents data recorded by Observer A, the dashed line represents Observer B, and the heavy solid line represents the photographic data obtained from the darkest area of the plume (10 arc minutes). Because of the separate viewing positions of the two observers and camera No. 2, the viewing aspects would be expected to become significantly different during the last two to three 5-second intervals of the run (approximately 5,000 ft range). Before that time, however, all transmission data should, ideally, be the same.

Although some similar trends can be seen by examining the photographic data and the observer data, differences between all three sources are

Run #6

Flight Profile: Overhead Pass
Approach Power

Fuel: JP-4

(Smoke #: 43)

Transmission @ 10 arc min: 1 - 95.8%
3 - 94.3%
6 - 93.0%
8 - 93.6%
10 - 96.4%

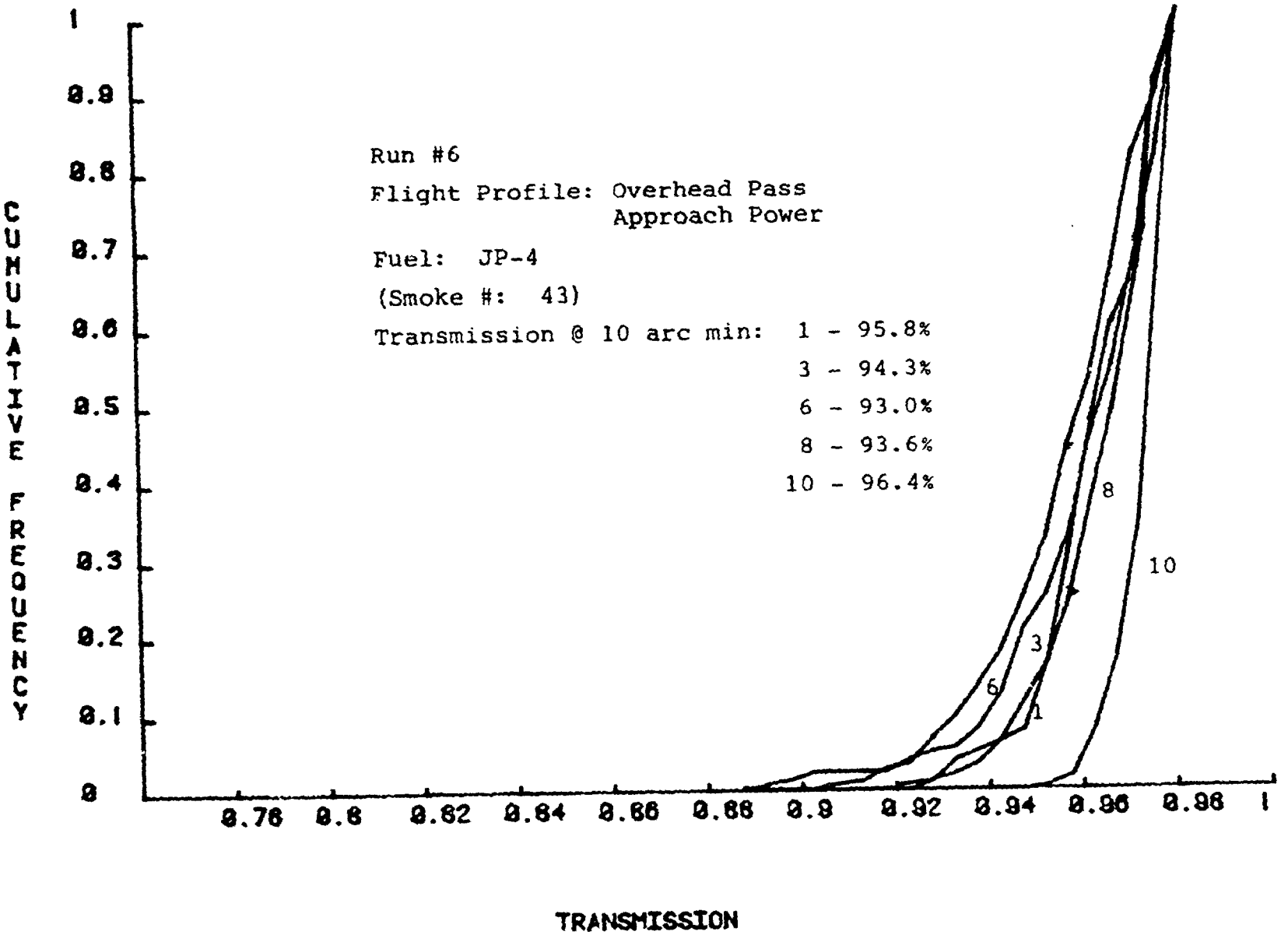

Figure 5-14. Transmission Cumulative Frequency for Run Number 6

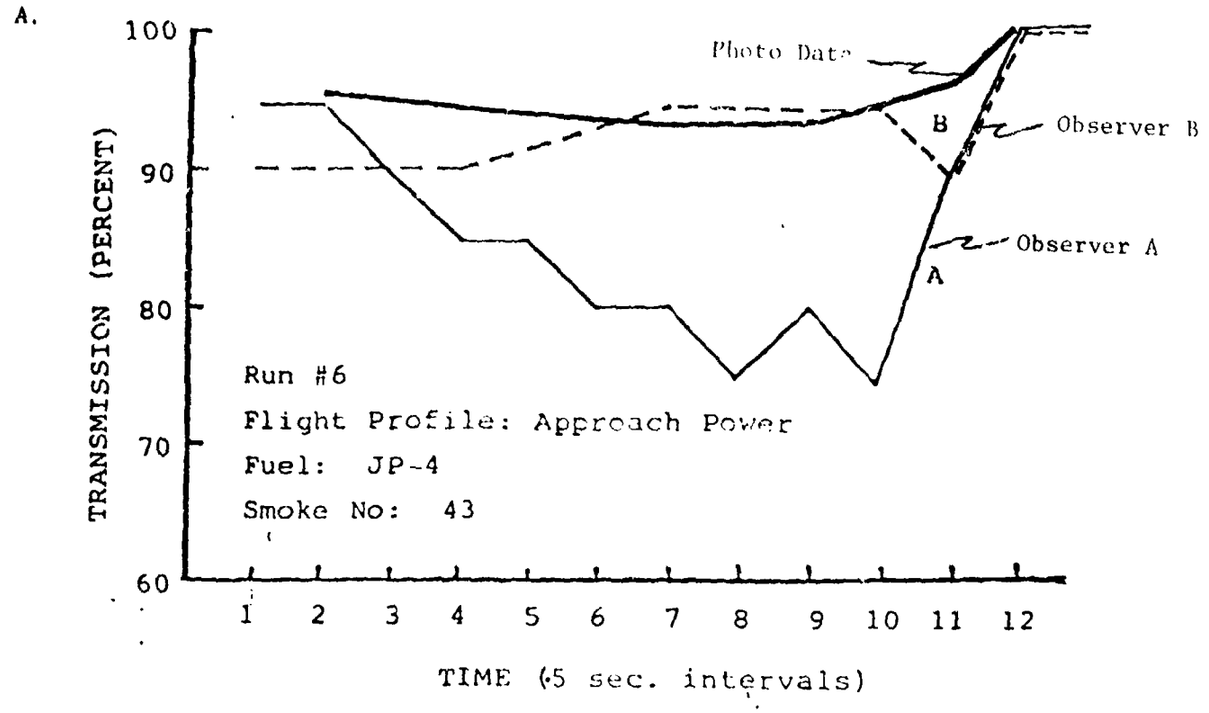

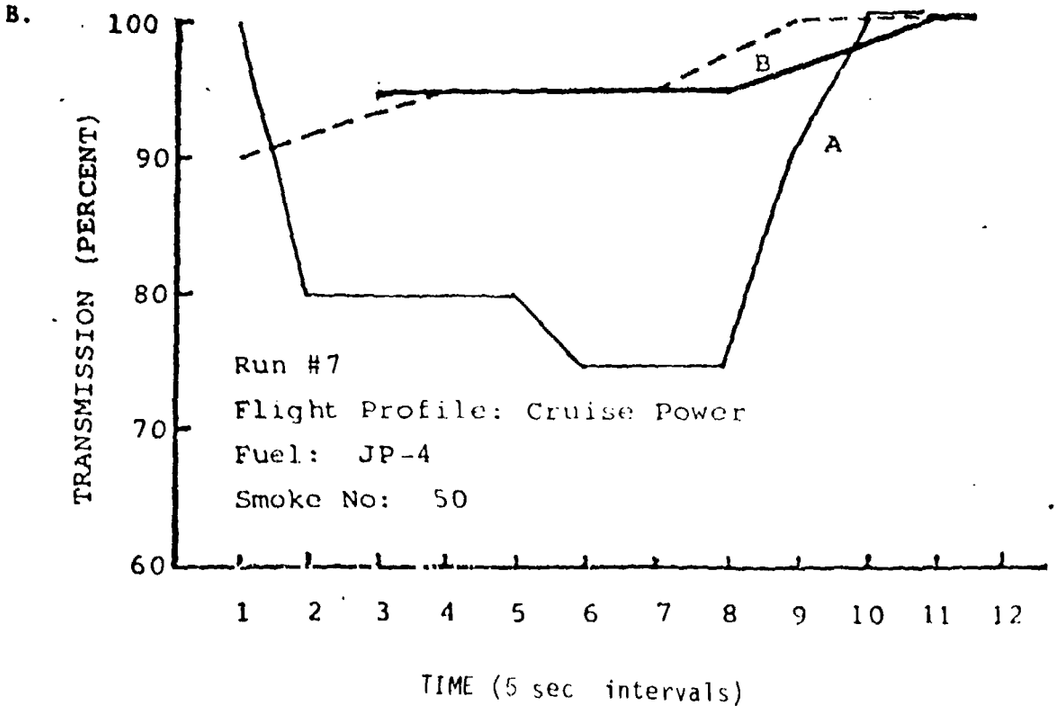

Figure 5-15. Transmission Data for Runs 6 and 7

evident. Figure 5-16 is a scatter diagram illustrating the transmission data measured photographically versus the observer readings. The data were plotted at each 5-second interval. Values were interpolated for time points where no readings were made. The dashed line illustrates exact correlation. The scatter of the data in the figure shows little correlation between the three data sources. Most of the transmission values for Observer A range between 70 and 85 percent and for Observer B range between 90 and 100 percent.

Although there are many problems related to the collection of good photographic data, the transmission of the plume at each pixel on the map is accurate at least within ± 2 standard deviations of the background brightness readings (using a 95-percent confidence level). The accuracy, therefore, in the transmision of each pixel is estimated to be better than ± 3 percent transmission. The accuracy (standard deviation) of the average or 10-arc minute transmission values is considerably better and is estimated to be less than ± 1 percent transmission. The methods selected for combining each value within the smoke plume to produce a single transmission value could introduce systematic errors in relating the photographic data to the observer readings.

5.6 COMPARISON OF PHOTOGRAPHIC TRANSMISSIONS WITH SMOKE NUMBER

Comparison of the photographic measurements of the smoke plume transmissions to the engine ground test Smoke Number (SN) at each power setting required the viewing aspect of the plume to be taken into account. To simplfy the task of evaluating the exact viewing angles of each plume photograph, the transmission data were grouped as a function of the slant range to the aircraft; and the viewing aspect was assumed to be the same within each group. The approximate slant range of the aircraft from each frame was determined by measurement of the wingspan from the photographic image. Table 5-8 summarizes the average plume transmission for several range groups and engine Smoke Numbers. The Smoke Numbers were determined from the ground run ups of one engine. The correlating factor between plume transmission and engine Smoke Number was the power setting used in each run.

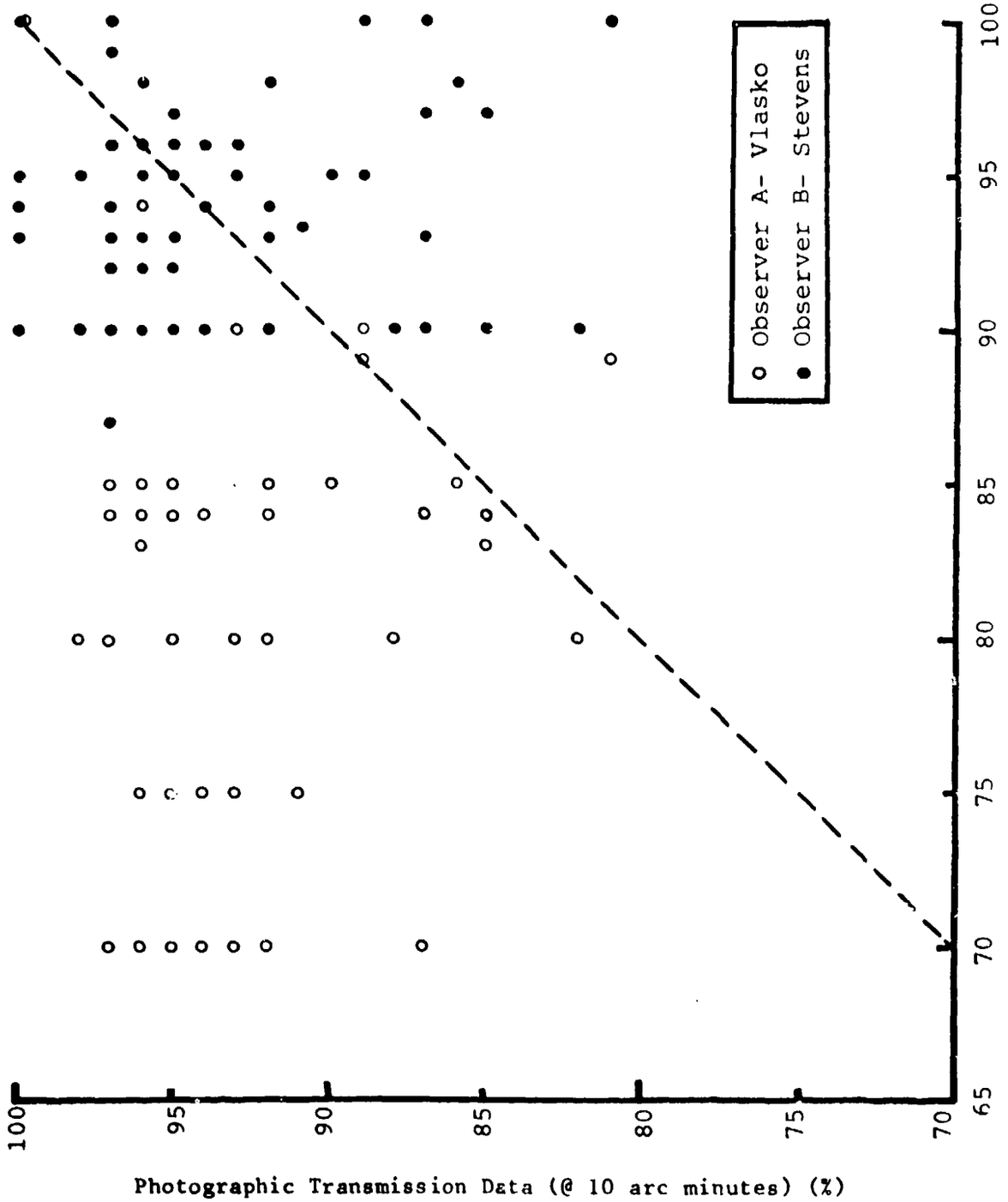

Figure 5-16 Photographic Versus Observer Data

TABLE 5-8. AVERAGE TRANSMISSION VERSUS SLANT RANGE

Run No.	5	6	7	8	9	11	12	13	14	15	16	18	20	21	22	23	24	25	26	27	28
Mode	FI	APR	CRU	CLB	TO	FI	APR	CRU	CLB	TO	FI	APR	CRU	CLB	TO	FI[1]	TO[2]	APR[3]	TO[4]	TO	TO
Fuel	JP-4										JP-5							Mixed[5]			
Smoke Number	44	43	50	51	51	44	43	50	51	51	54	54	60	60	60	54	60	54/43	60/51	60/51	60/51
Slant Range (1000's ft)	Average Transmission (% at various slant ranges)																				
16.0 - 20.5		96.6		97.7							97.8										
13.0 - 16.0	96	96.4	96.5		97.6	97	96.5		97.5	96.4		96.1	97.6			97.1		93.1	93.5	96.2	
10.0 - 13.0	98	97.7		97.8	95.6				96.5	97.5				96	96.3	95.4	92.6	95.1	94		96.9
7.0 - 10.0			96.4		97.2	97.3	96.5			97.9			96.6	96	97.1	94.4					
4.0 - 7.0			96.7	97	97.5		97.1	97.8	97.5	97.5	97.8	95.4	97.4			93.7	96.5	95.9	94.5		97.4
1.0 - 4.0			92.3	97.2	97.3	97.3	97.7	97.9	96.9		97.1	96.2	95.6			91.5	95	99.3	94.3	97.8	

KEY: FI - Flight Idle
APR - Approach
CRU - Cruise
CLB - Climb
TO - Takeoff

Notes:
(1) Flight Idle and Landing
(2) Takeoff and Climb
(3) Approach and Landing
(4) Takeoff and Climb
(5) JP-4 Left Side, JP-5 Right Side

The average plume transmission versus Smoke Number for slant ranges of 4,000 ft to 20,500 ft is plotted in Figure 5-17. The viewing elevation from the plume axis for these slant ranges varies from 1° to 7° while the viewing azimuth varies from 0° to 14°, i.e., the line of sight was nearly parallel to the exhaust plume path. The dashed lines on the diagram illustrate the upper and lower boundaries of the data. As illustrated by this envelope, the variability of the average transmission increases with an increase of the Smoke Number from 43 to 60 and precludes significant correlation between the transmission and Smoke Number. However, these boundaries were developed for the case where the observer's line-of-sight was nearly parallel to the exhaust plume path.

Consequently, any threshold of visibility correlation should be derived for broadside viewing, i.e., the observer's line of sight is perpendicular to exhaust plume. This criterion is supported by the results of Hoshizaki, et al., on jet aircraft plume visibility. (Reference 7) Their comprehensive study addressed plume geometry, smoke concentration in the plume, and the local extinction coefficient; such parameters as turbulent mixing, viewing angle, and smoke number were considered.

The photometric measurements show that when viewed normal to the exhaust stream, and where each engine can be viewed individually, the threshold of visibility corresponds to a Smoke Number of approximately 48. As previously stated, this is supported by the visual observations during the ground testing where the trained observers never saw the aircraft smoke plumes until the aircraft began its final approach. Then the plume became invisible again when the viewing angle approached 90 degrees. Since engine SN values varied from 43 to 60 during these observations, a Smoke Number value of 48 appears conservative.

An SN value of 48 which corresponds to the threshold of visibility was determined by using 98-percent transmission as the accepted threshold of opacity (Reference 37). Table 5-8 shows that the only large variations

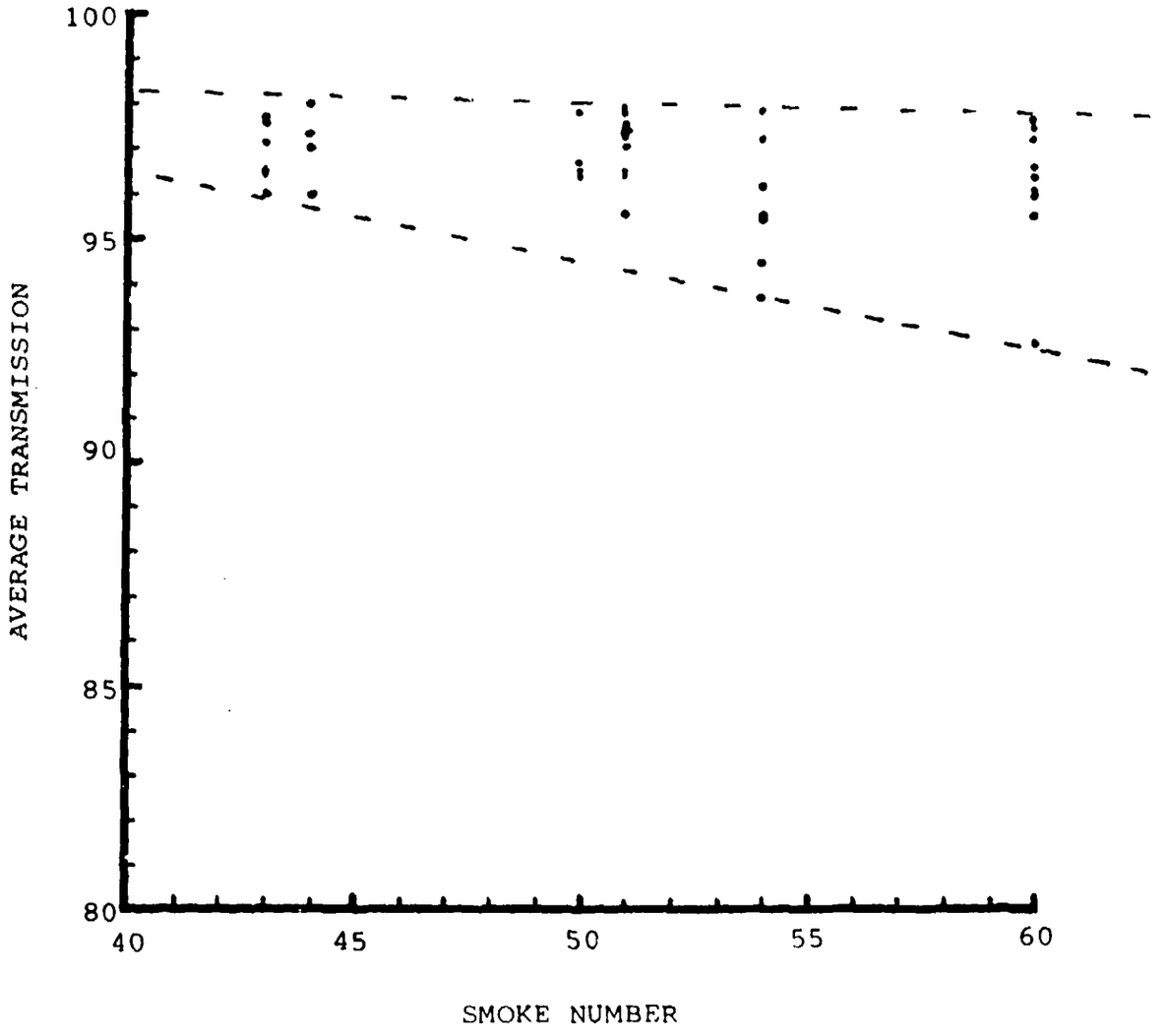

Figure 5-17 Average Transmission Versus Smoke Number

from this value exist for the higher Smoke Number runs. At aspect angles near 90° (broadside view) and hence shorter slant ranges, all transmissions values for the lower smoke cases are within the approximated 1-percent experimental error of being 98-percent transmissive.

Examination of the grey scale maps given earlier also supports the visible threshold value of SN = 48. In each case, the transmission of the plume either approaches 98-percent transmissiviity or is greater than 98 percent as the aspect angle approaches 90°, broadside viewing.

Further examination indicates that the total plume from all four engines has a complex interaction/dispersion behind the aircraft but that near the aircraft, each engine plume is not only independent of the others but also decreases in opacity with downstream distance.

REFERENCES

1. Military Specification MIL-E-8593, Engines, Aircraft, Turboshaft and Turboprop General Specification, 15 Oct 1975.

2. SAE Aerospace Recommended Practice 1179, Aircraft Gas Turbine Engine Exhaust Smoke Measurement, Society of Automotive Engineers, New York, NY, 4 May 1970 (Revised 6-15-80).

3. Military Specification MIL-T-5624, Turbine Fuel, Aviation, Grades JP-4 and JP-5.

4. "Control of Air Pollution from Aircraft and Aircraft Engines," Federal Register, Volume 38, Number 136, Part II, 17 July 1973.

5. "EPA Proposed Revisions to Gaseous Emissions Rules for Aircraft and Aircraft Engines," Federal Register, Volume 43, Number 58, 24 March 1978.

6. U. S. Environmental Protection Agency Office of Mobile Source Air Pollution Control, Report No. SDSB 79-25, Evaluation of Aircrft Smoke Standards for the Criterion of Invisibility by R. W. Munt, August 1979.

7. U.S. Air Force Wright Aeronuatical Report AFAPL-TR-76-29, Development of an Analytical Correlation Between Gas Turbine ENgine Smoke Production and Jet Plume Visibility, by H. Hoshizaki, A. D. Wood, S. Seidenstein, B. B. Brandolise, and J. W. Meyer, 31 July 1975 (Unclassified).

8. Charlson, R. J., "Atmospheric Visibility Related to Aerosol Mass Concentration," Env Sci Tech III (6), 540 (June 1969).

9. van de Hulst, H. C., Light Scattering by Small Particles, John Wiley and Sons, Inc., New York (1957).

10. Faxfog, F. R., Applied Optics XIII (8), 1913 (1974).

11. Charlson, R. J., and Alquist, N. C., Atmospheric Environment 3, (1969).

12. Mie, G., Ann Physik 25, 377 (1908).

13. Ensor, D. S., Charlson, R. J., Alquist, N. C., Whitby, K. T., Huser, R. B., and Liu, B. Y. H., "Multiwavelength Nephelometer Measurements in Los Angeles Smog Aerosol," in Aerosols and Atmospheric Chemistry, Hidy, G. M., (ed), Academic.

14. Wittig, S. L. K, Hireleman, E. D., Christiansen, J. V., "Noninterfering Optical Single Particle Counter Studies of Automobile Smoke Emissions," in Evaporation-Combustion of Fuel, Zung, J. T. (ed), Advanced in Chemistry Series #166, American Chemical Society.

15. Faxfog, F. R. and Roessler, D. M., Applied Optics, Vol. 17, p 2612, 1978.

16. Stockham, J., Fenton, D. L., Johnson, R., and Taubenkeil, L., Characterization of Aircraft Turbine Engine Particulate Emissions, Paper presented at 72nd Annual Meeting of Air Pollution Control Association, Cincinnati, OH, 24-29 June 1979.

17. Federal Aviation Administration, FAA-NA-71-24, Study of Visible Exhaust Smoke from Aircraft Jet Engines, Stockham, J., and Betz, H., 1971

18. U.S. Air Force Civil and Environmental Engineering and Development Office, TR-77-40, Smoke Abatement for DOD Test Cells, by B. C. Grems, 1977.

19. Champagne, D. L., Standard Measurement of Aircraft Gas Turbine Engine Exhuast Smoke, Americal Society of Mechanical Engineers Paper 71-GT-68.

20. McDonald, J. E., J Appl Meterology I, 391 (1962).

21. Stockham, J., and Bentz, H., Study of Visible Exhaust Smoke from Aircraft Jet Engines, Society of Automotive Engineers Paper 710428, May 1971.

22. U.S. Environmental Protection Agency, EPA-600/2-79-041, Chemical Composition of Exhaust Particulates from Gas Turbine Engines, by Robertson, D. J., Elwood, J. H., and Groth, R. H., February 1979.

23. Hodkinson, J. R., "The Optical Measurement of Aerosols," Optical Sciences, Davies, C. N. (ed), Academic Press, New York (1966).

24. A number of values have been suggested:

    a. index = 1.95 - 0.66i: Senftleben, H., and Benedict, E., Ann Phys Leipzig 54, 65 (1918)

    b. index = 1.8 - 0.6i, the average of the index for propane and acetylene soots: Dalzell, W. H., and Sarofin, A. F., J Heat Transfer 91, 100 (1969)

    c. index = 1.87 - 0.19i: Kunitomo, T., and Sato, T., Bull Japan Soc Mec Eng 14 58 (1971)

    d. index = 1.9 - 0.35i: Chippett, S., and Gray, W. A., Combustion Flame 31, 149 (1978)

25. Ensor, D. S., and Pilat, M. J., J Air Pol Control Assoc 21 (8), 496 (1971).

26. Thielke, J. F., and Pilat, M. J., Atmospheric Environment 12, 2439 (1978).

27. Wood, A. D., Correlation Between Smoke Measurements and the Optical Properties of Jet Engine Smoke, Society of Automotive Engineers Paper 751119 (1975).

28. Shaffernocker, W. M., and Stanforth, C. M., "Smoke Measurement Techniques," SAE Transactions 77, Paper 680346 (1968).

29. U.S. Environmental Protection Agency, EPA-650/2-75-055, Determination of Aircraft Turbine Engine Particulates, by K. M. Johansen and E. L. Kumm, (1975).

30. U.S. Air Force Wright Aeronautical Laboratories Report AFAPL-TR-74-64, Aircraft Exhaust Pollution and Its Affect on the U.S. Air Force, by W. S. Blazowski and R. E. Henderson, August 1974.

31. Ensor, D. S., and Pilat, M. J., Calculation of Smoke Plume Opacity from Particulate Air Pollutant Properties, Paper 70-83, Presented at the June 1970 Annual Meeeing of the Air Pollution Control Association, St. Louis, MO.

32. U. S. Department of Energy Report DOE/BETC/PPS-81/2, Aviation Turbine Fuels, by E. M. Shelton, 1980.

33. "Method 9 - Visual Determination of the Opacity of Emissions from Stationary Sources" Code of Federal Regulations, Title 40, Part 60, Appendix A.

34. U.S. Air Force Occupational and Environmental Health Laboratories, Report No. OEHL 80-27, Visual Opacity of C130H Turboprop Aircraft Edwards AFB, CA, by J. E. Stevens, 1980.

35. Weir, A., et. at., "Factors Influencing Plume Opacity," Environmental Science and Technology, 10 (6), 539, 1976.

36. Scipar, Inc., Report TR-8003, Photographic Smoke Analysis of the T56 Engine, by L. A. Mattison, D. J. Nixon and R. E. Kinzly, Dec. 1980.

37. Koschmeider, H., "Theorie der horizontalin Sichtweite," Beitr Phys frei Atmos 12 33-53, 171-181, 1924.

(The reverse of this page is blank.)

APPENDIX A

PARTICIPATING LABORATORIES AND ORGANIZATIONS

1. Environmental Sciences Branch, Air Force Engineering and Service Center Tyndall, AFB, Florida

2. Air Force Logistics Command, Wright Patterson AFB, Ohio

3. Detachment 4, 2762 Logistics Squadron, Air Force Logistics Command Ontario, California

4. Occupational and Environmental Health Laboratories, Brooks AFB, San Antonio, Texas

5. 6510th Test Wing, Air Force Flight Test Center, Edwards Air Force Base, California

6. Operations Test Center, Air Force Flight Test Center, Edwards AFB, California

7. Fuels and Lubricants Division, Aero Propulsion Laboratory, Air Force Wright Aeronautical Laboratories, Wright-Patterson AFB, Ohio

8. SCIPAR Incorporated, Buffalo, New York

9. Experimental Test Department, Detroit Diesel Allison Division, General Motors Corporation, Indianapolis, Indiana

10. Combustion Research and Development Section, Detroit Diesel Allison Division, General Motors Corporation, Indianapolis, Indiana

APPENDIX B

AIRCRAFT & ENGINE DATA

AIRCRAFT: Lockheed Transport Model C-130H (Hercules)

ENGINES: Allison Turboprop Model T56-A-15.

Installed Position:	1	2	3	4
Serial No.	AE109250	AE106872	AE109512	AE104249
Time (hours) at Start of Program:	4403.6	3549.7	2171.8	2688.4